5. Cyranoski, D. China spurs quest for human variome. *Nature* **469**, 455 (2011).
6. Byrne, B. J. *et al.* Pompe *disease*: design, methodology, and early findings from the Pompe registry. *Mol. Genet. Metab.* **103**, 1–11 (2011).
7. Rubinstein, Y. R. *et al.* Creating a global rare disease patient registry linked to a rare diseases biorepository database: Rare Disease-HUB (RD-HUB). *Contemp. Clin. Trials.* **31**, 394–404 (2010).
8. Forrest, C. B. *et al.* The case for a global rare disease registry. *Lancet* **377**, 1057–1059 (2011).
9. Abbott, A. Rare-disease project has global ambitions. *Nature* **472**, 17 (2011).
10. Cotton, R. G. *et al.* Capturing all disease-causing mutations for clinical and research use: toward an effortless system for the Human Variome Project. *Genet. Med.* **11**, 843–849 (2009).

Competing interests statement
The authors declare no competing financial interests.

FURTHER INFORMATION
The Human Genome Variation Society: www.hgvs.org
The Human Variome Project: www.humanvariomeproject.org
ALL LINKS ARE ACTIVE IN THE ONLINE PDF

CLINICAL REPORT

AMERICAN JOURNAL OF medical genetics PART A

Implantable Cardioverter Defibrillator for Progressive Hypertrophic Cardiomyopathy in a Patient With LEOPARD Syndrome and a Novel *PTPN11* Mutation Gln510His

Yasushi Wakabayashi,[1] Kyohei Yamazaki,[1] Yoko Narumi,[2] Satoshi Fuseya,[1] Miki Horigome,[1] Keiko Wakui,[2] Yoshimitsu Fukushima,[2] Yoichi Matsubara,[3] Yoko Aoki,[3] and Tomoki Kosho[2]*

[1]Department of Cardiovascular Internal Medicine, Prefectural Kiso Hospital, Kiso, Japan

[2]Department of Medical Genetics, Shinshu University School of Medicine, Matsumoto, Japan

[3]Department of Medical Genetics, Tohoku University School of Medicine, Sendai, Japan

Received 16 January 2011; Accepted 8 June 2011

LEOPARD syndrome (LS), generally caused by heterozygous mutations in the *PTPN11* gene, is a rare autosomal-dominant multiple congenital anomaly condition, characterized by skin, facial, and cardiac abnormalities. Prognosis appears to be related to the type of structural, myocardial, and arrhythmogenic cardiac disease, especially hypertrophic cardiomyopathy (HCM). We report on a woman with LS and a novel Gln510His mutation in *PTPN11*, who had progressive HCM with congestive heart failure and nonsustained ventricular tachycardia, successfully treated with implantable cardioverter defibrillator (ICD). Comparing our patient to the literature suggests that specific mutations at codon 510 in *PTPN11* (Gln510Glu, Gln510His, but not Gln510Pro) might be a predictor of fatal cardiac events in LS. Molecular risk stratification and careful evaluations for an indication of ICD implantation are likely to be beneficial in managing patients with LS and HCM. © 2011 Wiley-Liss, Inc.

Key words: LEOPARD syndrome; *PTPN11*; codon 510; hypertrophic cardiomyopathy; nonsustained ventricular tachycardia; implantable cardioverter defibrillator

How to Cite this Article:
Wakabayashi Y, Yamazaki K, Narumi Y, Fuseya S, Horigome M, Wakui K, Fukushima Y, Matsubara Y, Aoki Y, Kosho T. 2011. Implantable cardioverter defibrillator for progressive hypertrophic cardiomyopathy in a patient with LEOPARD syndrome and a novel *PTPN11* mutation Gln510His.
Am J Med Genet Part A 155:2529–2533.

INTRODUCTION

LEOPARD syndrome (LS) (OMIM#151100) is a rare autosomal-dominant multiple congenital anomaly condition, characterized by multiple lentigines, electrocardiographic (ECG) abnormalities, ocular hypertelorism, pulmonary stenosis, genital abnormalities, growth retardation, and sensorineural deafness [Sarkozy et al., 2008]. LS is caused by heterozygous missense mutations in the protein tyrosine phosphates, non-receptor type 11 gene (*PTPN11*) in roughly 85% of the cases [Digilio et al., 2002; Sarkozy et al., 2008]. The protein encoded by *PTPN11* functions as a cytoplasmic signaling transducer downstream of multiple receptors for growth factors, cytokines, and hormones, with a particular role through the RAS/mitogen activated protein kinase (MAPK) pathway [Sarkozy et al., 2008]. Disorders caused by mutations in various RAS/MAPK pathway components have recently been coined as "RASopathies", including Noonan syndrome, neurofibromatosis 1, cardio-facio-cutaneous syndrome, Costello syndrome, and LS [Rauen et al., 2010; Marin et al., 2011].

The prognosis of LS depends on the type of cardiovascular abnormality, especially hypertrophic cardiomyopathy (HCM) [Limongelli et al., 2008; Lehmann et al., 2009], however there have been few guidelines to manage complications. We report on a woman with LS and a novel Gln510His mutation in *PTPN11*, who had progressive HCM with congestive heart failure and nonsustained ventricular tachycardia, successfully treated with implantable cardioverter defibrillator (ICD) as for primary prevention of sudden death.

Grant sponsor: Ministry of Health, Labor and Welfare, Japan; Grant sponsor: Japan Society for the Promotion of Science.
*Correspondence to:
Tomoki Kosho, Department of Medical Genetics, Shinshu University School of Medicine, 3-1-1 Asahi, Matsumoto 390-8621, Japan.
E-mail: ktomoki@shinshu-u.ac.jp
Published online 9 September 2011 in Wiley Online Library (wileyonlinelibrary.com).
DOI 10.1002/ajmg.a.34194

CLINICAL REPORT

The proposita is a 38-year-old Japanese woman who underwent intracardiac repair of an atrial septal defect and pulmonary stenosis at age 2 years, when cardiac hypertrophy was detected. In childhood, she was easily exhausted after exercise and had growth retardation. At age 8 years, she was diagnosed with HCM with heart failure, though detailed laboratory data was not available. Oral administration of disopyramide and atenolol was initiated. In her 30s, she had generalized edema. Her plasma brain natriuretic peptide level was elevated at around 2,000 pg/ml (normal values, <18 pg/ml).

At age 37 years, she showed dyspnea, and was referred to our hospital. Her height was 143 cm (−3.0 SD) and weight was 40.8 kg (−1.6 SD). Her craniofacial features included hypertelorism, prominent eyes, a flat nose with anteverted nostrils, low-set posteriorly rotated ears, a long philtrum, thick lips, a high palate, and multiple caries (Fig. 1A). Her skeletal features included a short neck and short fingers with mild flexion contractures at the distal interphalangeal joints. She had numerous lentigines (congenital freckles) on the face (Fig. 1A) and café-au-lait spots on the back (Fig. 1B). She had no apparent hearing impairment. Her blood pressure was 130/66 mmHg, heart rate was 80 beats per minute, and SpO2 was 97% under administration of 1 L/min oxygen. Grade 2 systolic murmurs were heard at the 4th left intercostal space. The plasma brain natriuretic peptide level was 3,450 pg/ml. A chest radiograph showed cardiomegaly with a cardiothoracic ratio as 62% and pulmonary congestion. An ECG showed complete right bundle branch block and left axis deviation. Echocardiograph showed thickening of the interventricular septum as 23 mm (normal values, 7–12) and of the posterior wall of the left ventricle as 30 mm (normal values, 7–12), and tricuspid valve regurgitation with a pressure gradient as 35 mmHg. Pressure gradient of the left ventricular outlet was 21 mmHg at rest (stress echo was not performed to look for a provocable pressure gradient). Left ventricular end-diastolic volume was 20 ml (normal values, 56–136) and ejection fraction was 75% (normal values, >55). These findings were consistent with non-obstructive HCM with left ventricular hypertrophy and without low ejection fraction. The patient was treated with candesartan (angiotensin II receptor blocker), torasemide (diuretics), carvedilol (beta blocker), and amiodarone (antiarrhythmic agent), and her symptoms were improved with a decreased brain natriuretic peptide level to 1,720 pg/ml.

A delayed enhanced cardiac magnetic resonance imaging revealed severe concentric left ventricular hypertrophy with narrowing of the internal cavity and scattered hyper-enhancement regions that were suggested to be fibrosed myocardium [Moon et al., 2003]. A 24-hour Holter ECG showed 1,406 multifocal premature ventricular contractions and eight series of multifocal nonsustained ventricular tachycardia. An electrophysiological study, through a cardiac catheterization, demonstrated that polymorphic ventricular tachycardia was induced by programmed extrastimuli from the right ventricular apex with 400–250–240–230 ms, resulting in consciousness loss. According to the American College of Cardiology/the American Heart Association/the Heart Rhythm Society guidelines for device-based therapy [Epstein et al., 2008], she has two major risk factors (left ventricular wall thickness greater than or equal to 30 mm, nonsustained ventricular tachycardia on Holter ECG) for sudden death in HCM, and was considered to have a class IIa indication for ICD implantation. We placed ICD (Atlas™ + DR, St Jude Medical), which subsequently terminated several ventricular tachycardia episodes with anti-tachycardia pacing.

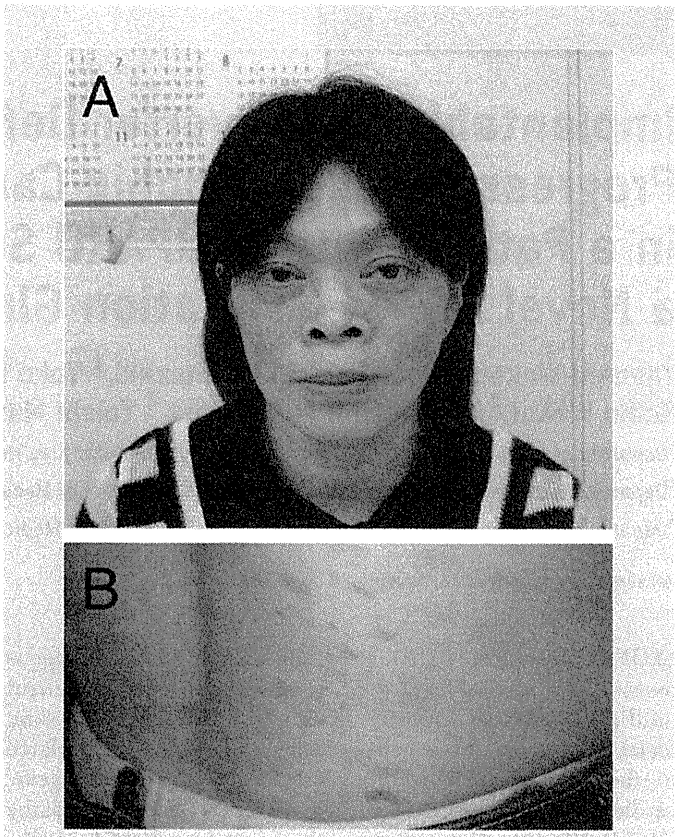

FIG. 1. Photographs of the patient at age 37 years. A: Craniofacial features. Hypertelorism, prominent eyes, a flat nose with anteverted nostrils, low-set posteriorly rotated ears, a long philtrum, thick lips, and multiple lentigines are noted, but typical adult Noonan syndrome-like features such as an inverted triangular shape with a pointed chin, a pinched nasal root, and prominent nasolabial folds are lacking. B: Café-au-lait spots on the back.

MUTATION ANALYSIS

Genomic DNA was isolated from the peripheral blood leukocytes of the patient. Each exon with flanking intronic sequences in *PTPN11* was amplified by polymerase chain reaction (PCR) with primers based on GenBank sequences. The primer sequences are available on request. PCR amplification was performed under standard condition using Taq DNA polymerase. After amplification, the PCR products were gel-purified and sequenced on an ABI PRISM 310 automated DNA sequencer (Applied Biosystems, California). A heterozygous missense mutation (c. 1,530 G > C; p. Gln510His) was identified in exon 13 (data not shown).

TABLE I. Patients With Mutations at Codon 510 of *PTPN11*

Family	1			2			3	4	5	6	7	8
Patient	**1**	**2**	**3**	**4**	**5**	**6**	**7**	**8**	**9**	**10**	**11**	**12**
Mutation		Gln510Pro			Gln510Pro		Gln510Glu	Gln510Glu	Gln510Glu	Gln510Glu	Gln510Glu	Gln510His
Sex	F	M	F	F	F	M	M	F	M	M	F	F
Age at publication (y, years; m, months)	?	12y	25y	?	?	4y	1y 3m	2y	2.3y	2m	37y	38y
Lentigines	+	+	+	+	+	−[a]	−	+	−	−	+	+
Café-au-lait spots	−	+	+					+	+	−		+
Congenital heart defects	−	+ (non-PS)	+ (PS, MVP)	−		+ (PS, ASD)	−	+ (MVA)	+ (PS)	+ (MR, VSD)	−	+ (PS, ASD)
Cardiomyopathy	−	−	−				HCM	HCM	HCM	HCM	HCM	HCM
ECG conduction abnormalities	?	+	−	+	−	+					+	+
Hypertelorism	−	−	−	+?	+	+	+	+	−	+	+	+
Prominent eyes									+	+		+
Ptosis	−	−	−					+	+			−
Low-set ears						+	+	+		+		+
Dysmorphic ears				+?	+	+	+	+	+	+		+
Hearing impairment	−	+	+	−	+	−	+	−	−	−	+	−
Genital abnormalities	−	C	−	−	−	−				C		
Scoliosis	−	−	−	−	+	−						
Coagulation abnormalies	−	+	+									
Growth retardation	−	−	−	+	−	+	−	+	+	−	+	+
Mental retardation	−	−	−			MDD	MDD	MDD	MDD			+
References	Keren et al. [2004]			Kalidas et al. [2005]			Takahashi et al. [2005]	Digilio et al. [2006]		Faienza et al. [2009]	Lehmann et al. [2009]	Present patient

Patient 1 was the mother of Patient 2 and Patient 3. Patient 4 and Patient 5 were the maternal grandmother and mother of Patient 6, respectively.
F, female; M, male; +, present; −, absent.
PS, pulmonary stenosis; MVP, mitral valve prolapse; ASD, atrial septal defect; MVA, mitral valve anomaly; MR, mitral valve regurgitation; VSD, ventricular septal defect; HCM, hypertrophic cardiomyopathy; C, cryptorchidism; MDD, motor developmental delay.
[a]absent at age 1 year.

DISCUSSION

This patient fulfills the clinical diagnostic criteria of LS proposed by Voron et al. [1976] with a novel heterozygous mutation Gln510His in *PTPN11*, the major causative gene for LS. *PTPN11* mutations in patients with LS are clustered in exons coding the protein tyrosine phosphatase domain, with two recurrent mutations in exons 7 (Tyr279Cys) and 12 (Thr468Met) in about 65% of *PTPN11*-positive cases, and other rare mutations [Digilio et al., 2002; Sarkozy et al., 2008]. Heterozygous missense mutations at codon 510 in exon 13 have been reported in 12 patients from eight families including this patient (Table I) [Keren et al., 2004; Kalidas et al., 2005; Takahashi et al., 2005; Digilio et al., 2006; Faienza et al., 2009; Lehmann et al., 2009]. A Gln510Glu mutation was found in five sporadic patients, who all manifested HCM with or without congenital heart defects. HCM was detected prenatally in two patients [Digilio et al., 2006], on the first day of life in one [Faienza et al., 2009], at age 1 month in one [Takahashi et al., 2005], and at age 23 years in one [Lehmann et al., 2009]. Pharmacotherapy including diuretics and propranolol was effective in two patients with progressive HCM with left ventricular outflow tract obstruction and congestive heart failure [Takahashi et al., 2005; Digilio et al., 2006; Limongelli et al., 2008]. Septal myectomy was required in one [Digilio et al., 2006; Limongelli et al., 2008] and sudden death occurred in one [Faienza et al., 2009]. On the other hand, a Gln510Pro mutation was found in six patients from two families, none of whom was described to manifest HCM, though three had congenital heart defects and two were elders at publication [Keren et al., 2004; Kalidas et al., 2005]. Limongelli et al. [2008] reviewed 24 LS patients with ($n = 16$) and without ($n = 8$) *PTPN11* mutations. They proposed mutations in exon 13 and codon 510 as molecular predictors of adverse cardiac events (life-threatening arrhythmic events, cardiac arrest, and heart failure), as well as LVH at ECG, New York Heart Association class >2, maximal wall thickness z-score $> +10$, LVOT gradient >50 mmHg, and NSVT as clinical predictors of these events. However, six patients from two families with a Gln510Pro mutation did not show HCM (Table I) [Keren et al., 2004; Kalidas et al., 2005]. Thus, presence of specific missense mutations at codon 510 (Gln510Glu and Gln510His, not Gln510Pro) would be a molecular risk factor of adverse cardiac events. The boys described by Takahashi et al. [2005] and Faienza et al. [2009] were diagnosed with Noonan syndrome because of no pigmented spots at the time of publication. They might develop lentigines and be diagnosed with LS, like the family described by Kalidas et al. [2005] (the 4-year-old boy showed no lentigines, while his mother and grandmother with the same mutation showed multiple lentigines).

Management of each "RASopathy" might depend on the cardiac phenotype. Whereas pulmonary valve stenosis with dysplastic leaflets and atrial/ventricular septal defects are the most prevalent cardiac defects in patients with Noonan syndrome caused by gain-of-function mutations in *PTPN11*, HCM is the most frequent cardiac complication and represents the only life-threatening problem in patients with LS caused by dominant-negative mutations in *PTPN11* [Sarkozy et al., 2008; Marin et al., 2011]. Indeed, the present patient could return to work under an appropriate cardiac management including intensive pharmacotherapy for controlling heart failure and ICD for preventing fatal arrhythmias. HCM in LS patients, which in general is asymptomatic and involves the left ventricle, is complicated by left ventricular outflow tract obstruction in up to 40% of the cases and frequently manifests during the second infancy before multiple lentigines occur [Sarkozy et al., 2008]. Therefore, those with LS, as well as those clinically diagnosed with Noonan syndrome and having HCM, are recommended to have molecular testing of *PTPN11* for genotype-based risk stratification of fatal cardiac events. LS patients with symptomatic HCM should receive intensive pharmacotherapy including beta blockers, calcium channel blockers, digoxin, diuretics, antiarrhythmic drugs, and angiotensin-converting enzyme inhibitors, depending on their symptoms and cardiac features; and for drug-refractory patients with obstructive HCM, surgical relief of left ventricular outflow obstruction is considered [Maron et al., 2003; Biagas and Hsu, 2006]. LS patients with symptomatic or asymptomatic HCM are recommended to have regular cardiac ultrasonography to measure left ventricular wall thickness and Holter ECG to detect nonsustained ventricular tachycardia for an indication of ICD implantation. Furthermore, etiology-based therapy might be realized, as recently published study by Marin et al. [2011], proposing effectiveness of TOR inhibitors such as rapamycin for the treatment of HCM in LS patients based on an evidence that dominant-negative *PTPN11* mutations in LS would enhance mTOR activity as critical for causing LS-associated HCM in a mouse model.

In conclusion, we have reported successful intervention through ICD implantation on a woman with LS and progressive HCM accompanied by congestive heart failure and nonsustained ventricular tachycardia, who was found to have a novel Gln510His mutation in *PTPN11*. Review of patients with mutations at codon 510 in *PTPN11* suggested that specific mutations (Gln510Glu, Gln510His, not Gln510Pro) would be a predictor of fatal cardiac events in LS. Molecular risk stratification and careful evaluations for an indication of ICD implantation are likely to be beneficial in managing patients with LS and HCM. Continued molecular characterization with cardiac phenotypes of these patients is crucial in further delineation of the risks as well as future etiology-based therapy.

ACKNOWLEDGMENTS

The authors are grateful to the patient for her cooperation. This work was supported by Research on Intractable Diseases, Ministry of Health, Labor and Welfare, Japan (to Y.F., Y.M., Y.A., T.K.), and Grants-in-Aids from the Japan Society for the Promotion of Science (to Y.M., Y.A.).

REFERENCES

Biagas K, Hsu DT. 2006. Cardiomyopathy. In: Nichols DG, Ungerleider RM, Spevak PJ, Greeley WJ, Cameron DE, Lappe DG, Wetzel RC, editors. Critical heart disease in infants and children, 2nd edition. Philadelphia: Mosby Elsevier. pp 981–993.

Digilio MC, Conti E, Sarkozy A, Mingarelli R, Dottorini T, Marino B, Pizzuti A, Dallapiccola B. 2002. Grouping of multiple-lentigines/LEOPARD and Noonan syndromes on the PTPN11 gene. Am J Hum Genet 71:389–394.

Digilio MC, Sarkozy A, Pacileo G, Limongeli G, Marino B, Dallapiccola B. 2006. PTPN11 gene mutations: Linking the Gln510Glu mutation to the "LEOPARD syndrome phenotype". Eur J Pediatr 165:803–805.

Epstein AE, DiMarco JP, Ellenbogen KA, Estes NA 3rd, Freedman RA, Gettes LS, Gillinov AM, Gregoratos G, Hammill SC, Hayes DL, Hlatky MA, Newby LK, Page RL, Schoenfeld MH, Silka MJ, Stevenson LW, Sweeney MO, Smith SC Jr, Jacobs AK, Adams CD, Anderson JL, Buller CE, Creager MA, Ettinger SM, Faxon DP, Halperin JL, Hiratzka LF, Hunt SA, Krumholz HM, Kushner FG, Lytle BW, Nishimura RA, Ornato JP, Page RL, Riegel B, Tarkington LG, Yancy CW, American College of Cardiology/American Heart Association Task Force on Practice Guidelines (Writing Committee to Revise the ACC/AHA/NASPE 2002 Guideline Update for Implantation of Cardiac Pacemakers and Antiarrhythmia Devices), American Association for Thoracic Surgery; Society of Thoracic Surgeons. 2008. ACC/AHA/HRS 2008 Guidelines for Device-Based Therapy of Cardiac Rhythm Abnormalities: A report of the American College of Cardiology/American Heart Association Task Force on Practice Guidelines (Writing Committee to Revise the ACC/AHA/NASPE 2002 Guideline Update for Implantation of Cardiac Pacemakers and Antiarrhythmia Devices) developed in collaboration with the American Association for Thoracic Surgery and Society of Thoracic Surgeons. J Am Coll Cardiol 51:e1–e62.

Faienza MF, Giordani L, Ferraris M, Bona G, Cavallo L. 2009. *PTPN11* gene mutation and severe neonatal hypertrophic cardiomyopathy: What is the link? Pediatr Cardiol 30:1012–1015.

Kalidas K, Shaw AC, Crosby AH, Newbury-Ecob R, Greenhalgh L, Temple IK, Law C, Patel A, Patton MA, Jeffery S. 2005. Genetic heterogeneity in LEOPARD syndrome: Two families with no mutations in *PTPN11*. J Hum Genet 50:21–25.

Keren B, Hadchouel A, Saba S, Sznajer Y, Bonneau D, Leheup B, Boute O, Gaillard D, Lacombe D, Layet V, Marlin S, Mortier G, Toutain A, Beylot C, Baumann C, Verloes A, Cavé H, For the French Collaborative Noonan Study Group. 2004. PTPN11 mutations in patients with LEOPARD syndrome: A French multicentric experience. J Med Genet 41:e117.

Lehmann LH, Schaeufele T, Buss SJ, Balanova M, Hartschuh W, Ehlermann P, Katus HA. 2009. A patient with LEOPARD syndrome and PTPN11 mutation. Circulation 119:1328–1329.

Limongelli G, Sarkozy A, Pacileo G, Calabro P, Digilio MC, Maddaloni V, Gagliardi G, Salvo GD, Iacomino M, Marino B, Dallapiccola B, Calabro R. 2008. Genotype-phenotype analysis and natural history of left ventricular hypertrophic in LEOPARD syndrome. Am J Med Genet Part A 146A:620–628.

Marin TM, Keith K, Davies B, Conner DA, Guha P, Kalaitzidis D, Wu X, Lauriol J, Wang B, Bauer M, Bronson R, Franchini KG, Neel BG, Kontaridis MI. 2011. Rapamycin reverses hypertrophic cardiomyopathy in a mouse model of LEOPARD syndrome-associated PTPN11 mutation. J Clin Invest 121:1026–1043.

Maron BJ, McKenna WJ, Danielson GK, Kappenberger LJ, Kuhn HJ, Seidman CE, Shah PM, Spencer WH 3rd, Spirito P, Ten Cate FJ, Wigle ED, Task Force on Clinical Expert Consensus Documents, American College of Cardiology, Committee for Practice Guidelines, European Society of Cardiology. 2003. American College of Cardiology/European Society of Cardiology clinical expert consensus document on hypertrophic cardiomyopathy. A report of the American College of Cardiology Foundation Task Force on Clinical Expert Consensus Documents and the European Society of Cardiology Committee for Practice Guidelines. J Am Coll Cardiol 42:1687–1713.

Moon JC, McKenna WJ, McCrohon JA, Elliott PM, Smith GC, Pennell DJ. 2003. Toward clinical risk assessment in hypertrophic cardiomyopathy with gadolinium cardiovascular magnetic resonance. J Am Coll Cardiol 41:1561–1567.

Rauen KA, Schoyer L, McCormick F, Lin AE, Allanson JE, Stevenson DA, Gripp KW, Neri G, Carey JC, Legius E, Tartaglia M, Schubbert S, Roberts AE, Gelb BD, Shannon K, Gutmann DH, McMahon M, Guerra C, Fagin JA, Yu B, Aoki Y, Neel BG, Balmain A, Drake RR, Nolan GP, Zenker M, Bollag G, Sebolt-Leopold J, Gibbs JB, Silva AJ, Patton EE, Viskochil DH, Kieran MW, Korf BR, Hagerman RJ, Packer RJ, Melese T. 2010. Proceedings from the 2009 genetic syndromes of the Ras/MAPK pathway: From bedside to bench and back. Am J Med Genet Part A 152A:4–24.

Sarkozy A, Digilio MC, Dallapiccola B. 2008. Leopard syndrome. Orphanet J Rare Dis 3:13.

Takahashi K, Kogaki S, Kurotobi S, Nasuno S, Ohta M, Okabe H, Wada K, Sakai N, Taniike M, Ozono K. 2005. A novel mutation in the PTPN11 gene in a patient with Noonan syndrome and rapidly progressive hypertrophic cardiomyopathy. Eur J Pediatr 164:497–500.

Voron DA, Hatfield HH, Kalkhoff RK. 1976. Multiple lentigines syndrome. Case report and review of the literature. Am J Med 60:447–456.

Journal of Human Genetics (2011) 56, 707–715

www.nature.com/jhg

ORIGINAL ARTICLE

HRAS mutants identified in Costello syndrome patients can induce cellular senescence: possible implications for the pathogenesis of Costello syndrome

Tetsuya Niihori[1], Yoko Aoki[1], Nobuhiko Okamoto[2], Kenji Kurosawa[3], Hirofumi Ohashi[4], Seiji Mizuno[5], Hiroshi Kawame[6], Johji Inazawa[7], Toshihiro Ohura[8], Hiroshi Arai[9], Shin Nabatame[10], Kiyoshi Kikuchi[11], Yoshikazu Kuroki[12], Masaru Miura[13], Toju Tanaka[14], Akira Ohtake[15], Isaku Omori[16], Kenji Ihara[17], Hiroyo Mabe[18], Kyoko Watanabe[19], Shinichi Niijima[20], Erika Okano[21], Hironao Numabe[22] and Yoichi Matsubara[1]

Costello syndrome (CS) is a congenital disease that is characterized by a distinctive facial appearance, failure to thrive, mental retardation and cardiomyopathy. In 2005, we discovered that heterozygous germline mutations in *HRAS* caused CS. Several studies have shown that CS-associated *HRAS* mutations are clustered in codons 12 and 13, and mutations in other codons have also been identified. However, a comprehensive comparison of the substitutions identified in patients with CS has not been conducted. In the current study, we identified four mutations (p.G12S, p.G12A, p.G12C and p.G12D) in 21 patients and analyzed the associated clinical manifestations of CS in these individuals. To examine functional differences among the identified mutations, we characterized a total of nine HRAS mutants, including seven distinct substitutions in codons 12 and 13, p.K117R and p.A146T. The p.A146T mutant demonstrated the weakest Raf-binding activity, and the p.K117R and p.A146T mutants had weaker effects on downstream c-Jun N-terminal kinase signaling than did codon 12 or 13 mutants. We demonstrated that these mutant HRAS proteins induced senescence when overexpressed in human fibroblasts. Oncogene-induced senescence is a cellular reaction that controls cell proliferation in response to oncogenic mutation and it has been considered one of the tumor suppression mechanisms *in vivo*. Our findings suggest that the *HRAS* mutations identified in CS are sufficient to cause oncogene-induced senescence and that cellular senescence might therefore contribute to the pathogenesis of CS.
Journal of Human Genetics (2011) **56**, 707–715; doi:10.1038/jhg.2011.85; published online 18 August 2011

Keywords: Costello syndrome; HRAS; phenotype-genotype; RAS/MAPK; senescence

INTRODUCTION

Costello syndrome (CS, OMIM 218040) is a genetic disorder that is characterized by a distinctive facial appearance, loose skin, failure to thrive, mental retardation, cardiomyopathy and a predisposition to tumor formation.[1] Patients with CS have an estimated 13% chance of developing tumors, usually rhabdomyosarcoma, neuroblastoma or bladder cancer.[2] Previously, we identified heterozygous germline *HRAS* mutations in patients with CS.[3] It has been suggested that the CS diagnosis should be applied only to patients with a mutation in *HRAS* because of the high risk of malignancies associated with *HRAS* mutations and the relative homogeneity of the CS phenotype.[4]

[1]Department of Medical Genetics, Tohoku University School of Medicine, Sendai, Japan; [2]Department of Medical Genetics, Osaka Medical Center and Research Institute for Maternal and Child Health, Izumi, Japan; [3]Division of Medical Genetics, Kanagawa Children's Medical Center, Yokohama, Japan; [4]Division of Medical Genetics, Saitama Children's Medical Center, Saitama, Japan; [5]Department of Pediatrics, Central Hospital, Aichi Human Service Center, Kasugai, Japan; [6]Department of Genetic Counseling, Ochanomizu University, Tokyo, Japan; [7]Department of Molecular Cytogenetics, Medical Research Institute and School of Biomedical Science, Tokyo Medical and Dental University, Tokyo, Japan; [8]Division of Pediatrics, Sendai City Hospital, Sendai, Japan; [9]Department of Pediatric Neurology, Morinomiya Hospital, Osaka, Japan; [10]Department of Child Neurology, National Center Hospital (NCH), National Center of Neurology and Psychiatry, Tokyo, Japan; [11]Department of Pediatrics, Shimane Prefectural Central Hospital, Izumo, Japan; [12]Department of Neonatology, Kurashiki Central Hospital, Kurashiki, Japan; [13]Division of Cardiology, Tokyo Metropolitan Children's Medical Center, Tokyo, Japan; [14]Division of Clinical Genetics and Molecular Medicine, National Research Institute for Child Health and Development, Tokyo, Japan; [15]Department of Pediatrics, Saitama Medical University, Moroyama, Japan; [16]Department of Neonatology, Center for Maternal, Fetal & Neonatal Medicine, Tokyo Metropolitan Bokutoh Hospital, Tokyo, Japan; [17]Department of Pediatrics, Graduate School of Medical Sciences, Kyushu University, Fukuoka, Japan; [18]Department of Child Development, Faculty of Life Sciences, Kumamoto University, Kumamoto, Japan; [19]Division of Pediatrics, National Hospital Organization Kokura Medical Center, Kitakyushu, Japan; [20]Department of Pediatrics, Juntendo University, Nerima Hospital, Tokyo, Japan; [21]Department of Pediatrics, Jikei University School of Medicine, Tokyo, Japan and [22]Department of Clinical Genetics, Kyoto University Hospital, Kyoto, Japan

Correspondence: Dr T Niihori or Dr Y Aoki, Department of Medical Genetics, Tohoku University School of Medicine, 1-1 Seiryo-machi, Sendai 980-8574, Japan.
E-mail: tniihori@med.tohoku.ac.jp or aokiy@med.tohoku.ac.jp
Received 4 April 2011; revised and accepted 15 June 2011; published online 18 August 2011

A total of 14 *HRAS* missense mutations and one duplication mutation have been reported in 185 patients with CS[3,5–23] or congenital myopathy with excess of muscle spindles.[24] Most of these mutations have previously been reported as somatic and oncogenic mutations in various tumors. More than 90% of the mutations found in CS patients are clustered in codons 12 and 13 (p.G12A/S/V/C/D/E and p.G13C/D). Other mutations, including p.Q22K, p.E37dup, p.T58I, p.E63K, p.K117R, p.A146V and p.A146T, have also been identified, albeit rarely. Although the clinical manifestations of CS appear to be homogeneous, several genotype-phenotype correlations have been reported. Previous studies have also suggested that CS patients with the p.G12A mutation may have an increased risk of malignancy, compared with patients with p.G12S.[7] Patients with the p.G12C mutation had a more severe CS phenotype; these individuals developed severe hypertrophic cardiomyopathy and died in the neonatal period. Patients with p.K117R or p.A146V had a milder and more unusual CS phenotype, compared with patients with mutations in codon 12 or 13. Though detailed analyses of some mutants have been performed,[13,25–28] a comprehensive comparison of the substitutions identified in patients with CS has not been conducted.

The activated RAS/mitogen-activated protein kinase (MAPK) pathway generally stimulates cell proliferation, but it can also result in antiproliferation under certain conditions. Overexpressing HRAS p.G12V in human and murine fibroblasts caused oncogene-induced senescence (OIS),[29–31] which protects cells from proliferating in the presence of oncogene-induced damage.[32,33] OIS is a cellular reaction that controls cell proliferation in response to oncogenic mutation and is considered a tumor suppression mechanism *in vivo*.[34,35] Studies of a zebrafish model of CS, which expresses *HRAS* p.G12V, have shown that progenitor cells in the adult heart and brain undergo cellular senescence, suggesting that OIS in adult progenitor cells contributes to the development of CS. We hypothesized that OIS would be a key mechanism of the clinical manifestations in patients with CS, including short stature, osteoporosis and tumor suppressive effects. However, it has not been verified that HRAS mutants other than p.G12V cause cellular senescence.

The three aims of this study were the following: (1) to examine the detailed clinical manifestations of CS in patients with *HRAS* mutations, (2) to characterize a large panel of HRAS mutants to look for differences among various mutations located in codon 12/13 and to compare the effects of mutants in codon 12/13 with those of p.K117R/p.A146T, and (3) to clarify whether *HRAS* mutants other than p.G12V can cause OIS. To address these issues, we analyzed the *HRAS* mutations in CS patients and studied the Raf-binding activity, downstream signaling and ability to cause senescence of a large panel of HRAS mutants.

MATERIALS AND METHODS

Patients

A total of 31 patients suspected of having CS were recruited to the study. The diagnosis of CS was evaluated by clinical geneticists. All patients had sporadic cases. The study was approved by the Ethics Committee of the Tohoku University School of Medicine.

Mutation analysis

We sequenced the *HRAS* genes of all patients in the study to confirm the diagnosis of CS. After obtaining written informed consent, genomic DNA was isolated from the peripheral leukocytes of patients. Four coding exons of *HRAS* from 31 CS patients were sequenced. Each *HRAS* exon with flanking intronic sequences was amplified using primers based on sequences obtained from GenBank (GenBank accession no. NT035113). The M13 reverse or forward sequence was added to the 5′ end of the polymerase chain reaction primers for use, as a sequencing. polymerase chain reaction was performed in a 30 µl reaction containing 10 mM Tris-HCl (pH 8.3), 50 mM KCl, 1.5 mM $MgCl_2$, 0.2 mM deoxyribonucleotide triphosphate, 10% (v/v) dimethyl sulfoxide, 0.4 pmol each primer, 100 ng genomic DNA and 2.5 units of Taq DNA polymerase. The reaction consisted of 35 cycles of denaturation at 94 °C for 15 s, annealing at 57 °C for 15 s and extension at 72 °C for 30 s. The products were gel-purified and sequenced on an Applied Biosystems 3130 Genetic Analyzer (Applied Biosystems, Foster City, CA, USA).

Plasmids

To introduce exogenous wild-type or mutated HRAS into cultured cells, we constructed plasmids encoding wild-type or mutant *HRAS* cDNAs. Human *HRAS* cDNA in pUSEamp was purchased from Upstate Biotechnology (Lake Placid, NY, USA). The plasmid was digested with *Eco*RI and subcloned into pBluescript KSII+ (Stratagene, La Jolla, CA, USA). Substitutions generating p.G12V (c.35G>T), p.G12A (c.35G>C), p.G12S (c.34G>A), p.G12C (c.34G>C), p.G12D (c.35G>A), p.G13C (c.37G>C), p.G13D (c.38G>A), p.K117R (c.350A>G) or p.A146T (c.436G>A) were introduced using the QuikChange Site-Directed mutagenesis kit (Stratagene). All mutant and wild-type constructs were verified by sequencing. The full-length wild-type and mutant *HRAS* cDNAs were digested with *Eco*RI and subcloned into the pBabe-puro retroviral vector (GenHunter, Nashville, TN, USA) and the pCAGGS expression vector (gifted by Dr Jun-ichi Miyazaki of Osaka University). The pBabe-zeo-Ecotropic Receptor plasmid (Addgene plasmid 10687, Addgene Inc., Cambridge, MA, USA) was obtained from Addgene.

Cell culture and senescence-associated β-galactosidase staining

NIH 3T3 cells, human fibroblast BJ cells and the Phoenix Ampho and Eco packaging cell lines were purchased from the American Tissue Culture Collection (Manassas, VA, USA). NIH 3T3 cells were maintained in Dulbecco's modified Eagle medium containing 10% calf serum, 100 U/ml penicillin and 100 µg/ml streptomycin. BJ and Phoenix cells were maintained in Dulbecco's modified Eagle medium containing 10% fetal calf serum, 100 U/ml penicillin and 100 µg/ml streptomycin. To characterize the phenotypes of cells overexpressing wild-type or mutated HRAS, senescence associated β-galactosidase staining was performed with the Senescence β-Galactosidase Staining Kit (Cell Signaling Technology, Beverly, MA, USA) according to the manufacturer's protocol.

Ras activation assay

We performed RAS activation assays to clarify the functional differences among the HRAS mutants identified in patients with CS. The Ras activation assay kit was purchased from Millipore (Billerica, MA, USA). NIH 3T3 cells were plated in 6-well plates at 1.5×10^5 cells per well. Cells were transfected using Lipofectamine Plus (Invitrogen, Carlsbad, CA, USA) with 1 µg wild-type or mutant *HRAS* construct. The assay was performed according to the manufacturer's protocol.

Luciferase assay

We used luciferase assays to examine the effect of the identified mutations on the RAS pathway. NIH 3T3 cells were plated in 12-well plates at 1×10^5 cells per well. After 24 h, cells were transiently transfected with 700 ng pFR-luc, 10 ng pFA2-Elk1 or 10 ng pFA2-cJun, 7 ng phRLnull-luc and 35 ng wild-type or mutant *HRAS* construct, using Lipofectamine Plus (Invitrogen). At 18 h after transfection, the cells were serum starved in Dulbecco's modified Eagle medium for 24 h. Cells were then harvested in passive lysis buffer, and luciferase activity was assayed using the Promega Dual-Luciferase assay kit (Promega, Madison, WI, USA). Renilla luciferase expressed by phRLnull-luc was used to normalize the transfection efficiency. The experiments were performed in triplicate. Statistical analysis was performed with Tukey's multiple comparison test.

Western blotting

We performed western blotting against molecular markers of premature senescence to confirm their expression in cells overexpressing HRAS. Cells were harvested at the indicated times, washed in ice-cold phosphate-buffered saline and lysed on ice in lysis buffer (10 mM Tris-HCl, pH 7.5 and 1% sodium

dodecyl sulfate). Lysates were boiled for 5 min and centrifuged at 13 000 *g* for 10 min at 4 °C. Protein concentrations were estimated using the Lowry or Bradford method (BioRad, Hercules, CA, USA), and each lysate was adjusted to equalize the protein concentrations. Equal volumes of lysates were mixed with 2×sodium dodecyl sulfate sample buffer and boiled for 5 min. Electrophoresis was performed on 5–15% sodium dodecyl sulfate–polyacrylamide gels. After separation, proteins were transferred to nitrocellulose membranes. The membranes were blocked in 5% non-fat dry milk in Tris-buffered saline with 0.1% Tween 20 for 1 h at room temperature and incubated overnight at 4 °C with one of the following primary antibodies: HRAS (sc-520, Santa Cruz Biotechnology, Santa Cruz, CA, USA), phospho-p44/42MAPK, p44/42MAPK (#9102 and #9101, respectively, Cell Signaling Technology, Danvers, MA, USA), p16 (sc-468, Santa Cruz Biotechnology), phospho-p53 (Ser15) (#9284, Cell Signaling Technology) or β-actin (A5316, Sigma, St. Louis, MO, USA). Detection was performed using the enhanced chemiluminescence method (Amersham, GE Healthcare UK, Amersham, UK), with the appropriate peroxidase-conjugated secondary antibody.

Retroviral gene transfer

We generated cells that stably overexpressed wild-type or mutant HRAS by retroviral gene transfer. Phoenix cells (5×10^6) were plated in a 10 cm dish, incubated for 24 h and then transfected with 18 μg of retroviral plasmid using Fugene6 (Roche Applied Science, Mannheim, Germany). After 48 h, the virus-containing medium was filtered through a 0.45-μm filter and supplemented with 4 μg/ml polybrene (Sigma) to collect the virus (first supernatant). Viruses were collected after an additional 24 h as before (second supernatant). BJ fibroblasts were plated at 6×10^5 cells per 10 cm dish and incubated overnight. For infections, the culture medium was replaced with the first viral supernatant and incubated at 37 °C for 8 h, after which the second viral supernatant was added. Infected cell populations were selected 40 h later, using 2 μg/ml puromycin or 200 μg/ml zeocin. The ecotropic retrovirus receptor was introduced into the BJ human fibroblasts by infecting cell populations with an amphotropic vector (pBabe-zeo-ecotropic receptor produced in Phoenix Ampho cells), allowing subsequent infection with ecotropic viruses.

RESULTS

Mutation analysis in patients with CS

Genomic sequencing analysis of 32 individuals with confirmed or suspected CS revealed four different missense mutations in 21 patients: a heterozygous 34G>A mutation (p.G12S) in 16 patients, a heterozygous 35G>C mutation (p.G12A) in three patients, a heterozygous 34G>T change (p.G12C) in one patient, and a 35G>A change (p.G12D) in one patient.

The clinical data for 21 CS mutation-positive patients are shown in Table 1. Curly and/or sparse hair (21/21), failure to thrive (21/21), coarse facial appearance (20/20), deep palmar/planter creases (20/21), soft, loose skin (18/21) and relative macrocephaly (17/21) were observed at high frequency in patients with CS, as previously reported.[1,3] Laryngomalacia (soft larynx), which has been reported in several patients with CS,[36–38] was observed in three patients. One patient had hypertension, which was also observed in a mouse model of CS.[39] One patient had glycogen storage disease type III, as previously reported by Kaji *et al.*,[40] accompanied by a p.G12S mutation. Bladder cancer was observed in one patient.

One patient (NS 223) with *HRAS* p.G12C had severe clinical manifestations of CS and was treated with pravastatin.[41] She was born at 23 weeks of gestation with extremely low birth weight (766 g, >90th percentile), even though her mother had received tocolytic therapy. Her Apgar scores were 3 and 7 at 1 and 5 min, respectively. She required mechanical ventilation. Extubation was attempted periodically beginning at day 70, but it was unsuccessful until she turned 2 years old, because of her laryngomalacia and increased mucus secretion. Hypertrophic cardiomyopathy was first observed on day 38. The patient was given propranolol and cibenzoline to control the gradual progression of hypertrophic cardiomyopathy. Cardiac arrest after extubation occurred on day 192 and the patient was successfully resuscitated. Papillomas developed at approximately 11 months of age. Erosion and itching of skin were not well controlled by topical steroids or antihistamines. Pravastatin (0.2 ~ 0.4 mg/kg/day) was administered in anticipation of its suppressive effect on RAS, beginning when she was 16 months old. Thereafter, the papillomas disappeared once and appeared again, but were less numerous than when they first appeared. The effects of pravastatin on hypertrophic cardiomyopathy were not obvious. The patient was discharged from the hospital at 2 years of age.

Analysis of mutant HRAS activation states and effects on the downstream pathway

We performed RAS activation assays to elucidate functional differences among the mutants identified in patients with CS. We transfected NIH 3T3 cells with wild-type *HRAS* or one of the nine *HRAS* mutants identified in patients with CS. We found an increase in guanosine triphosphate (GTP)-bound HRAS in all cells transfected with *HRAS* p.G12V, p.G12A, p.G12S, p.G12C, p.G12D, p.G13C, p.G13D, p.K117R and p.A146T. We did not detect any differences among the increases of GTP-bound HRAS in the cells transfected with *HRAS* p.G12V, p.G12A, p.G12S, p.G12C, p.G12D, p.G13C, p.G13D and p.K117R. The increase in the level of GTP-bound HRAS-p.A146T was milder than that of other mutants.

Next, we examined the effect of the identified mutations on the RAS pathway by studying the activation of ELK1 and c-Jun in transfected NIH 3T3 cells. ELK1 and c-Jun are the main nuclear targets of extracellular signal-regulated kinase and c-Jun N-terminal kinase, respectively. We transfected the pFR-luc trans-reporter vector, the pFA2-ELK1 or pFA2-cJun vector and the phRLnull-luc vector into NIH 3T3 cells and determined the relative luciferase activity (RLA) in each cell line. The basal RLA in cells transfected with active MEK1 or MEKK constructs showed a three-fold increase, compared with cells transfected with wild-type *HRAS* cDNA (Figure 1a). A significant increase in RLA was observed upon transfection with ELK1 and HRAS p.G12V, p.G12A, p.G12S, p.G12C, p.G12D, p.G13C, p.G13D, p.K117R and p.A146T (Figure 1b). The RLA of c-Jun was significantly increased in cells transfected with HRAS p.G12V, p.G12A, p.G12S, p.G12C, p.G12D, p.G13C and p.G13D (Figure 1c). In these assays with ELK1 and c-Jun, we observed no significant difference among RLAs in the cells transfected with *HRAS* p.G12V, p.G12A, p.G12S, p.G12C, p.G12D, p.G13C and p.G13D. These results suggest that HRAS-p.K117R and p.A146T had a weaker effect on the c-Jun N-terminal kinase pathway than the other mutants.

Cellular senescence in human fibroblasts transfected with HRAS mutants

The HRAS p.G12V mutant causes a senescence phenotype when transduced into human diploid fibroblasts. To examine the ability of the various mutants identified in patients with CS to cause senescence, we introduced wild-type or mutated *HRAS* cDNAs into human fibroblast BJ cells, using retroviral gene transfer. Figure 2a shows these cells six days after infection. Wild-type HRAS-induced cells exhibited a narrow and elongated morphology and they were not flat like senescent cells. They proliferated at levels similar to cells transfected with empty vector. In contrast, the p.G12V, p.G12A, p.G12S, p.G12C, p.G12D, p.G13C, p.G13D, p.K117R and p.A146T mutants produced cells with a senescence phenotype, exhibiting flat, enlarged and multivacuolated morphology and prominent nucleoli. Senescence

Table 1 Clinical findings and *HRAS* mutations in our CS patients

Patients	*NS71*	*NS123*	*NS125*	*NS132*	*NS137*	*NS139*	*NS156*	*NS157*	*NS167*	*NS181*	*NS198*	*NS217*
Gender	F	F	F	F	M	F	M	F	M	M	M	M
Age	9 months	11 years	17years	3 years	10 years	7 months	2 years 3 months	17 years	3 months	3 years	1 year 2 months	4 years 6 months
Paternal age at birth (years)	39	29	42	37	30	35	34	34	37	33	31	40
Maternal age at birth (years)	28	26	27	31	28	35	36	36	34	33	31	37
Growth and development												
Postnatal failure to thrive	+	+	+	+	+	+	+	+	+	+	+	+
Mental retardation	+	+	+	+	+	+	+	+	+	+	+	+
Craniofacial characteristics												
Relative macrocephaly	+	+	+	+	+	+	+	+	+	+	+	+
Coarse facial appearance	+	+	+	+	+	+	+	+	+	+	+	+
Muscloskeltal characteristics												
Short neck	+	+	+	+	+	+	+	+	–	+	–	+
Hyperextensive fingers	+	+	+	+	–	+	+	+	+	–	–	–
Tight Achilles tendon	–	+	+	+	+	–	+	–	–	–	–	+
Abnormal foot position	+	+	+	+	NA	+	NA	–	–	+	–	+
Skin characteristics												
Curly, sparse hair	+	+	+	+	+	+	+	+	+	+	Curly	+
Soft, loose skin	+	+	+	+	+	+	+	+	–	+	+	+
Deep palmer/ planter creases	+	+	+	+	+	+	+	+	+	+	+	+
Cardiac defect												
Hypertrophic cardiomyopathy	+	–	+	–	+	+	NA	+	–	+	–	–
Others	PS	–	–	–	–	–	PAC	Anomalous septum in the right atrium	VSD, arrhythmia	Atrial tachycardia	–	ASD, PSVT, PVC, CAR
Neoplasia												
Papillomata	–	–	+	–	–	–	NA	+	+	–	+	–
Other tumors		Bladder cancer							Heart neoplasia			
Others			GH deficiency		GSDIII	Chiari I, syringomyelia	Pyrolic stenosis	Congenial stridor, GH deficiency	Hypoplastic nails	Hypertention		Hydronephrosis, GER, laryngomalacia
HRAS mutation												
Nucleotide substitution	c.34G>A	c.35G>C	c.34G>A	c.34G>A	c.34G>A	c.34G>A	c.34G>A	c.34G>A	c.34G>A	c.34G>A	c.34G>A	c.34G>A
Amino acid substitution	p.G12S	p.G12A	p.G12S	p.G12S	p.G12S	p.G12S	p.G12S	p.G12S	p.G12S	p.G12S	p.G12S	p.G12S

Table 1 Continued

Patients	*NS223*	*NS231*	*NS239*	*NS248*	*NS254*	*NS263*	*NS299*	*NS318*	*NS324*	*Total*
Gender	F	F	M	M	F	M	F	F	F	
Age	6 months	5 months	18 years	5 years	2 months	1 month	3 years	1 month	1 year 6 months	
Paternal age at birth (years)	34	27	27	NA	37	35	34y	33	33	
Maternal age at birth (years)	36	27	26	30	34	36	35y	32	33	
Growth and development										
Postnatal failure to thrive	+	+	+	+	+	+	+	+	+	21/21
Mental retardation	+	+	+	+	NA	+	+	+	+	20/20
Craniofacial characteristics										
Relative macrocephaly	–	+	+	–	+	+	–	–	+	17/21
Coarse facial appearance	+	+	+	+	+	+	+	+	+	21/21
Muscloskeltal characteristics										
Short neck	–	+	NA	NA	+	+	+	–	–	14/19
Hyperextensive fingers	–	+	–	+	+	–	–	+	+	13/21
Tight Achilles tendon	+	NA	–	+	–	–	–	+	+	10/20
Abnormal foot position	–	–	NA	NA	NA	–	–	+	+	9/16
Skin characteristics										
Curly, sparse hair	+	Curly	Curly	+	+	+	Curly	+	Curly	21/21
Soft, loose skin	–	+	+	+	+	+	–	+	+	18/21
Deep palmer/planter creases	+	–	+	+	+	+	+	+	+	20/21
Cardiac defect										
Hypertrophic cardiomyopathy	+	–	+	+	+	+	+	+	+	14/20
Other	PAC	PVC	–	–	–	–	–	PAC	PAC	
Neoplasia										
Papillomata	+	–	+	–	–	–	–	–	–	6/20
Other tumors										
Others	Prabastatin administration	Laryngomalasia, hydrocephallus	GH deficiency, Arnold Chiari, scoliosis	Empty sella, GH deficiency, hypothyroidism, hypogonadism, syringomyelia		Hyperinsulinemia		Laryngomalasia seizure	Laryngomalasia	
HRAS mutation										
Nucleotide substitution	c.34G>T	c.35G>A	c.34G>A	c.34G>A	c.34G>A	c.35G>C	c.34G>A	c.35G>C	c.34G>A	
Amino acid substitution	p.G12C	p.G12D	p.G12S	p.G12S	p.G12S	p.G12A	p.G12S	p.G12A	p.G12S	

Abbreviations: –, absent; +, present; ASD, atrial septal defect; F, female; GER, gastroesophageal relfux; GH, growth hormone; GSDIII, glycogen storage disease III; M, male; NA, not available; PAC, premature atrial contraction; PS, pulmonic stenosis; PSVT, paroxysmal supraventricular tachycardia; PVC, premature ventricular contraction; VSD, ventricular septal defect.

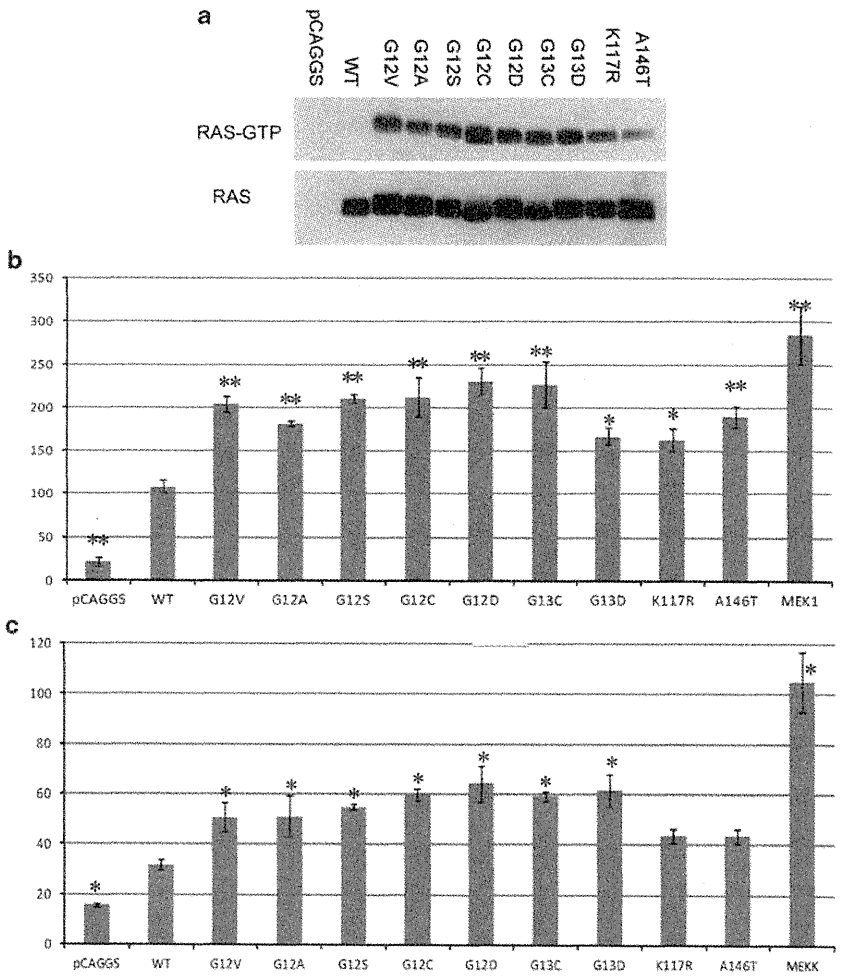

Figure 1 Functional characterization of HRAS mutants. (**a**) Ras-guanosine triphosphate (GTP) in NIH 3T3 cells transfected with wild-type or mutant HRAS constructs. HRAS protein levels were similar in NIH3T3 cells expressing each protein and were subsequently used as a loading control. (**b**, **c**) Stimulation of ELK (**b**) and c-Jun (**c**) transcription by *HRAS* mutants. The ELK-and c-Jun-GAL4 vectors and GAL4-luciferase trans-reporter vector were transiently co-transfected with various *HRAS* constructs into unstimulated NIH 3T3 cells. Relative luciferase activity (RLA) was normalized to the activity of a co-transfected control vector (phRLnull-luc) expressing *Renilla reniformis* luciferase. The results are expressed as the means and s.d. from triplicate samples. MEK1 and MEKK were used as positive controls. WT, wild type. $^{*}P<0.05$; $^{**}P<0.01$ compared with WT.

associated β-galactosidase staining confirmed that these cells showed cellular senescence.

Two downstream signaling pathways, p53 and Rb-p16, are activated during cellular senescence. To examine oncogene induced cellular senescence at the molecular level, we assessed senescence markers, including phosphorylated extracellular signal-regulated kinase, phosphorylated p53 and p16, in cells expressing HRAS mutant proteins (Figure 2b). As expected, phosphorylated p53 (Ser15) and p16 levels, as well as phospho-extracellular signal-regulated kinase levels, were significantly increased in the cells transfected with HRAS mutants relative to cells transfected with mock vector or wild-type HRAS. These results demonstrate that not only p.G12V, but also the other eight CS-related HRAS mutants, can cause OIS.

DISCUSSION

In this study, we identified four *HRAS* mutations in 21 patients with CS and evaluated their detailed clinical manifestations of the disease in these patients. Biochemical analyses, including a GTP binding assay and luciferase assays to detect ELK and c-Jun trans-activation, showed that there were no significant differences among the analyzed mutations in codon 12/13. The p.A146T mutant demonstrated the weakest Raf binding activity, and the p.K117R and p.A146T mutants had weaker effects on downstream c-Jun N-terminal kinase signaling than mutants in codon 12 or 13. Our results indicated that all HRAS mutants detected in CS patients were able to cause OIS.

Our study is the first to demonstrate that HRAS mutants other than p.G12V can induce senescence when they are overexpressed in human fibroblasts. The symptoms of CS seem to be caused by either hyperproliferation or hypoproliferation, coupled with growth factor resistance, which may be ascribable to DNA damage response or OIS. Postnatal cerebellar tonsillar herniation, Chiari 1 malformation,[42] deep palmar and plantar creases and papillomata may all be caused by hyperproliferation. In contrast, the poor weight gain, short stature and endocrine dysfunction observed in CS patients[43–45] might be caused by hypoproliferation. Adult brain and heart progenitor cells in a zebrafish CS model with a homozygous HRAS p.G12V mutation

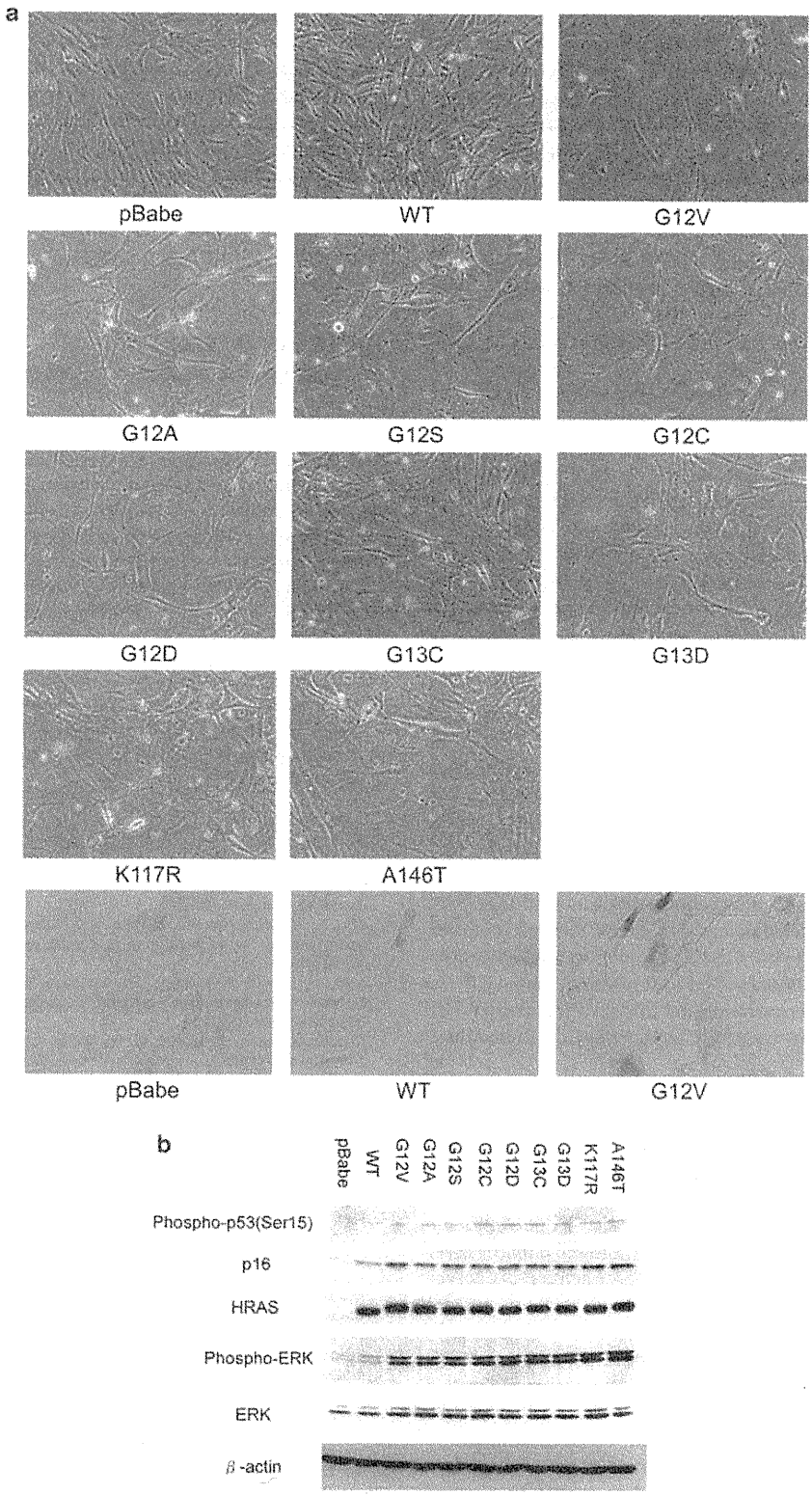

Figure 2 Effect of Costello syndrome (CS)-associated HRAS mutants on primary fibroblasts. (**a**) BJ cells transduced with retroviruses expressing wild-type or mutant HRAS. Images in the lowest tier show senescence-associated β-galactosidase staining. (**b**) Immunoblots of cellular lysates from BJ cells transduced with empty vector (pBabe) or with wild-type or mutant HRAS retroviruses.

exhibited cellular senescence, suggesting that the age-related worsening of the Costello phenotype[46] might occur, because the replicative capability of adult progenitor cells is exhausted. Osteoporosis has frequently been found in adult patients with CS,[47] suggesting that cellular senescence affects osteogenesis. However, further studies will be needed to determine whether OIS indeed contributes to the pathogenesis in patients with CS.

It has been suggested that clinical symptoms vary among patients with mutations in codon 12 or 13. In previous studies, a total of 19 CS patients have been reported to die from severe cardiomyopathy, cardiac arrhysmia, rhabdomyosarcoma, respiratory failure, multi-organ failure or sepsis. The number of fatal cases was 5/138 patients with p.G12S, 4/6 with p.G12C, 3/17 with p.G12A, 3/4 with p.G12D, 2/2 with p.G12V, 1/1 with p.G12E and 1/1 with p.E63K.[3,5–23] The mortality of patients with p.G12C or p.G12D was significantly higher than that of the patients with the more common p.G12S (P=0.026 by Fisher's exact test). Previous studies have shown that the p.G12V substitution has the highest transformative potential (p.G12V > p.G12A, p.G12S, p.G12C, p.G12D > p.G13D) and is the most frequently found mutation in human tumors.[48,49] However, our Ras activity assays and luciferase assays did not show any differences among *HRAS* codon 12/13 mutants. This may be due to the extremely high expression level of HRAS protein in our transient transfection study, which could make it difficult to detect subtle differences between mutants. Further studies will be necessary to clarify whether the high mortality in patients with p.G12C or p.G12D is due to functional differences in these mutants or due to bias because of our small sample size of patients.

Mutations at codons 117 and 146 are rare in CS and somatic cancers. Meanwhile, mutations at codons G12, G13 and Q61 have been shown to impair intrinsic and GTPase activating protein-mediated GTP hydrolysis, leading to elevated levels of cellular RAS-GTP. It has been reported that the nucleotide exchange rate of both p.K117R and p.A146V HRAS is increased, relative to wild type.[13,27,28] However, the transformational potential of p.A146V HRAS is partially activated,[27] whereas that of p.K117R-HRAS is not; its transformational activity is instead similar to that of GTPase impaired mutants.[28] Our results and those of other reports suggest that p.K117R and p.A146T have milder effects on downstream effectors than do mutations in codon 12/13.

The clinical manifestations of CS in patients with p.K117R or p.A146V mutations suggest that these alleles have distinct effects, compared with mutations in codon 12/13. Of two CS patients with a p.K117R mutation, one patient had an atypical phenotype such as microretrognatism and slightly less-pronounced plantar and palmar creases.[7] The other patient had mild craniofacial manifestations of CS.[13] One patient with the p.A146V mutation showed a mildly coarse face and did not have deep palmar creases.[6] These atypical phenotypes might be attributed to the mild effects of p.K117R or p.A146V compared with codon 12/13 mutants.

Inhibitors of the RAS/MAPK pathway could provide benefits for patients with RAS/MAPK syndromes. Statins are 3-hydroxy-3-methyl-glutaryl-CoA reductase inhibitors that result in decreased isoprenylation of RAS[50] and are now widely used for the treatment of hyperlipidemia. Statins have been used to modify the clinical manifestation of neurofibromatosis type I, which is caused by a genetic defect in a negative regulator of the RAS/MAPK pathway. Studies using mouse models of NF1 (Nf1 mice) have shown that treatment with a statin reverses the cognitive deficits of these mice.[51] A randomized control trial for neurofibromatosis type I treatment with simvastatin had a negative outcome.[52] Furthermore, statins have displayed antitumor activity in experimental tumor models, though clinical antitumor effects of statins have not been established.[53] Well-designed clinical studies will be needed to determine the effects of statins or other RAS inhibitors on manifestations of CS.

In conclusion, we identified *HRAS* mutations in 21 patients and examined the clinical manifestations of mutation-positive patients. Functional analysis revealed that CS-causing mutant HRAS proteins caused OIS in human fibroblasts. These findings may help enable more accurate prognoses for patients with *HRAS* mutations and contribute to our understanding of the mechanism underlying CS pathogenesis.

CONFLICT OF INTEREST

The authors declare no conflict of interest.

ACKNOWLEDGEMENTS

We thank the patients who participated in this study and their families and doctors, including Naoki Watanabe and Tomohiro Iwasaki, who referred the cases. We are grateful to Dr Garry Nolan of Stanford University for supplying Phoenix-Eco and Ampho cells, to Dr William C Hahn for supplying the pBabe-zeo-ecotropic receptor vector, and to Dr Jun-ichi Miyazaki of Osaka University for supplying the pCAGGS expression vector. We are also grateful to Drs Noriko Ishida and Keiko Nakayama for their technical assistance with the infection of retroviral vectors. We thank Kumi Kato and Hasumi Haba for their technical assistance. This work was supported by Grants-in-Aids for young scientists (A and S) from the Ministry of Education, Culture, Sports, Science and Technology of Japan (nos. 19689022, 21689029 and 19679005) to TN and YA, the Science and Technology Foundation of Japan Grant-in-Aid for Scientific Research to TN, and the Ministry of Health, Labour and Welfare to YM and YA.

1 Hennekam, R. C. Costello syndrome: an overview. *Am. J. Med. Genet. C. Semin. Med. Genet.* **117C,** 42–48 (2003).
2 Aoki, Y., Niihori, T., Narumi, Y., Kure, S. & Matsubara, Y. The RAS/MAPK syndromes: novel roles of the RAS pathway in human genetic disorders. *Hum. Mutat.* **29,** 992–1006 (2008).
3 Aoki, Y., Niihori, T., Kawame, H., Kurosawa, K., Ohashi, H., Tanakam, Y. *et al.* Germline mutations in HRAS proto-oncogene cause Costello syndrome. *Nat. Genet.* **37,** 1038–1040 (2005).
4 Kerr, B., Allanson, J., Delrue, M. A., Gripp, K. W., Lacombe, D., Lin, A. E. *et al.* The diagnosis of Costello syndrome: nomenclature in Ras/MAPK pathway disorders. *Am. J. Med. Genet. A* **146A,** 1218–1220 (2008).
5 Estep, A. L., Tidyman, W. E., Teitell, M. A., Cotter, P. D. & Rauen, K. A. HRAS mutations in Costello syndrome: detection of constitutional activating mutations in codon 12 and 13 and loss of wild-type allele in malignancy. *Am. J. Med. Genet. A.* **140,** 8–16 (2006).
6 Gripp, K. W., Lin, A. E., Stabley, D. L., Nicholson, L., Scott, C. I. Jr, Doyle, D. *et al.* HRAS mutation analysis in Costello syndrome: genotype and phenotype correlation. *Am. J. Med. Genet. A.* **140,** 1–7 (2006).
7 Kerr, B., Delrue, M. A., Sigaudy, S., Perveen, R., Marche, M., Burgelin, I. *et al.* Genotype-phenotype correlation in Costello syndrome: HRAS mutation analysis in 43 cases. *J. Med. Genet.* **43,** 401–405 (2006).
8 van Steensel, M. A., Vreeburg, M., Peels, C., van Ravenswaaij-Arts, C. M., Bijlsma, E., Schrander-Stumpel, C. T. *et al.* Recurring HRAS mutation G12S in Dutch patients with Costello syndrome. *Exp. Dermatol.* **15,** 731–734 (2006).
9 Gripp, K. W., Lin, A. E., Nicholson, L., Allen, W., Cramer, A., Jones, K. L. *et al.* Further delineation of the phenotype resulting from BRAF or MEK1 germline mutations helps differentiate cardio-facio-cutaneous syndrome from Costello syndrome. *Am. J. Med. Genet. A.* **143A,** 1472–1480 (2007).
10 Orstavik, K. H., Tangeraas, T., Molven, A. & Prescott, T. E. Distal phalangeal creases—a distinctive dysmorphic feature in disorders of the RAS signalling pathway? *Eur. J. Med. Genet.* **50,** 155–158 (2007).
11 Sovik, O., Schubbert, S., Houge, G., Steine, S. J., Norgard, G., Engelsen, B. *et al.* *De novo* HRAS and KRAS mutations in two siblings with short stature and neuro-cardio-facio-cutaneous features. *J. Med. Genet.* **44,** e84 (2007).
12 Zampino, G., Pantaleoni, F., Carta, C., Cobellis, G., Vasta, I., Neri, C. *et al.* Diversity parental germline origin, and phenotypic spectrum of *de novo* HRAS missense changes in Costello syndrome. *Hum. Mutat.* **28,** 265–272 (2007).
13 Denayer, E., Parret, A., Chmara, M., Schubbert, S., Vogels, A., Devriendt, K. *et al.* Mutation analysis in Costello syndrome: functional and structural characterization of the HRAS pLys117Arg mutation. *Hum. Mutat.* **29,** 232–239 (2008).

14 Gripp, K. W., Innes, A. M., Axelrad, M. E., Gillan, T. L., Parboosingh, J. S., Davies, C. *et al.* Costello syndrome associated with novel germline HRAS mutations: an attenuated phenotype? *Am. J. Med. Genet. A.* **146A,** 683–690 (2008).
15 Hou, J. W. Rapidly progressive scoliosis after successful treatment for osteopenia in Costello syndrome. *Am. J. Med. Genet. A.* **146,** 393–396 (2008).
16 Limongelli, G., Pacileo, G., Digilio, M. C., Calabro, P., Di Salvo, G., Rea, A. *et al.* Severe, obstructive biventricular hypertrophy in a patient with Costello syndrome: clinical impact and management. *Int. J. Cardiol.* **130,** e108–e110 (2008).
17 Schulz, A.L., Albrecht, B., Arici, C., van der Burgt, I., Buske, A., Gillessen-Kaesbach, G. *et al.* Mutation and phenotypic spectrum in patients with cardio-facio-cutaneous and Costello syndrome. *Clin. Genet.* **73,** 62–70 (2008).
18 Gremer, L., De Luca, A., Merbitz-Zahradnik, T., Dallapiccola, B., Morlot, S., Tartaglia, M. *et al.* Duplication of Glu37 in the switch I region of HRAS impairs effector/GAP binding and underlies Costello syndrome by promoting enhanced growth factor-dependent MAPK and AKT activation. *Hum. Mol. Genet.* **19,** 790–802 (2010).
19 Kuniba, H., Pooh, R.K., Sasaki, K., Shimokawa, O., Harada, N., Kondoh, T. *et al.* Prenatal diagnosis of Costello syndrome using 3D ultrasonography amniocentesis confirmation of the rare HRAS mutation G12D. *Am. J. Med. Genet. A.* **149A,** 785–787 (2009).
20 Lin, A. E., O'Brien, B., Demmer, L. A., Almeda, K. K., Blanco, C. L., Glasow, P. F. *et al.* Prenatal features of Costello syndrome: ultrasonographic findings and atrial tachycardia. *Prenat. Diagn.* **29,** 682–690 (2009).
21 Piccione, M., Piro, E., Pomponi, M. G., Matina, F., Pietrobono, R., Candela, E. *et al.* A premature infant with Costello syndrome due to a rare G13C HRAS mutation. *Am. J. Med. Genet. A.* **149A,** 487–489 (2009).
22 Sol-Church, K., Stabley, D. L., Demmer, L. A., Agbulos, A., Lin, A. E., Smoot, L. *et al.* Male-to-male transmission of Costello syndrome: G12S HRAS germline mutation inherited from a father with somatic mosaicism. *Am. J. Med. Genet. A.* **149A,** 315–321 (2009).
23 Zhang, H., Ye, J. & Gu, X. Recurring G12S mutation of HRAS in a Chinese child with Costello syndrome with high alkaline phosphatase level. *Biochem. Genet.* **47,** 868–871 (2009).
24 van der Burgt, I., Kupsky, W., Stassou, S., Nadroo, A., Barroso, C., Diem, A. *et al.* Myopathy caused by HRAS germline mutations: implications for disturbed myogenic differentiation in the presence of constitutive HRas activation. *J. Med. Genet.* **44,** 459–462 (2007).
25 McGrath, J. P., Capon, D. J., Goeddel, D. V. & Levinson, A. D. Comparative biochemical properties of normal and activated human ras p21 protein. *Nature.* **310,** 644–649 (1984).
26 Al-Mulla, F., Milner-White, E. J., Going, J. J. & Birnie, G. D. Structural differences between valine-12 and aspartate-12 Ras proteins may modify carcinoma aggression. *J. Pathol.* **187,** 433–438 (1999).
27 Feig, L. A. & Cooper, G. M. Relationship among guanine nucleotide exchange, GTP hydrolysis, and transforming potential of mutated ras proteins. *Mol. Cell. Biol.* **8,** 2472–2478 (1988).
28 Der, C. J., Weissman, B. & Macdonald, M. J. Altered guanine-nucleotide binding and H-Ras transforming and differentiating activities. *Oncogene.* **3,** 105–112 (1988).
29 Sikora, E., Arendt, T., Bennett, M. & Narita, M. Impact of cellular senescence signature on ageing research. *Ageing Res. Rev.* **10,** 146–152 (2010).
30 Serrano, M., Lin, A. W., McCurrach, M. E., Beach, D. & Lowe, S. W. Oncogenic ras provokes premature cell senescence associated with accumulation of p53 and p16INK4a. *Cell* **88,** 593–602 (1997).
31 Narita, M., Nunez, S., Heard, E., Narita, M., Lin, A. W., Hearn, S. A. *et al.* Rb-mediated heterochromatin formation and silencing of E2F target genes during cellular senescence. *Cell* **113,** 703–716 (2003).
32 Di Micco, R., Fumagalli, M., Cicalese, A., Piccinin, S., Gasparini, P., Luise, C. *et al.* Oncogene-induced senescence is a DNA damage response triggered by DNA hyper-replication. *Nature* **444,** 638–642 (2006).
33 Bartkova, J., Rezaei, N., Liontos, M., Karakaidos, P., Kletsas, D., Issaeva, N. *et al.* Oncogene-induced senescence is part of the tumorigenesis barrier imposed by DNA damage checkpoints. *Nature* **444,** 633–637 (2006).
34 Narita, M. & Lowe, S. W. Senescence comes of age. *Nat. Med.* **11,** 920–922 (2005).
35 Campisi, J. Suppressing cancer: the importance of being senescent. *Science* **309,** 886–887 (2005).
36 Kawame, H., Matsui, M., Kurosawa, K., Matsuo, M., Masuno, M., Ohashi, H. *et al.* Further delineation of the behavioral and neurologic features in Costello syndrome. *Am. J. Med. Genet. A.* **118A,** 8–14 (2003).
37 Kalfa, D., Fraisse, A. & Kreitmann, B. Medical and surgical perspectives of cardiac hypertrophy in Costello syndrome. *Cardiol. Young* **19,** 644–647 (2009).
38 Digilio, M. C., Sarkozy, A., Capolino, R., Chiarini Testa, M. B., Esposito, G., de Zorzi, A. *et al.* Costello syndrome: clinical diagnosis in the first year of life. *Eur. J. Pediatr.* **167,** 621–628 (2008).
39 Schuhmacher, A. J., Guerra, C., Sauzeau, V., Canamero, M., Bustelo, X. R. & Barbacid, M. A mouse model for Costello syndrome reveals an Ang II-mediated hypertensive condition. *J. Clin. Invest.* **118,** 2169–2179 (2008).
40 Kaji, M., Kurokawa, K., Hasegawa, T., Oguro, K., Saito, A., Fukuda, T. *et al.* A case of Costello syndrome and glycogen storage disease type III. *J. Med. Genet.* **39,** E8 (2002).
41 Omori, I., Shimizu, M. & Watanabe, T. An infant with Costello syndrome and a rare HRAS mutation (G12C). *J. Jpn. Pediatr. Soc.* **114,** 1592–1597 (2010).
42 Gripp, K. W., Hopkins, E., Doyle, D. & Dobyns, W.B. High incidence of progressive postnatal cerebellar enlargement in Costello syndrome: brain overgrowth associated with HRAS mutations as the likely cause of structural brain and spinal cord abnormalities. *Am. J. Med. Genet. A.* **152A,** 1161–1168 (2010).
43 Gregersen, N. & Viljoen, D. Costello syndrome with growth hormone deficiency and hypoglycemia: a new report and review of the endocrine associations. *Am. J. Med. Genet. A.* **129A,** 171–175 (2004).
44 Stein, R. I., Legault, L., Daneman, D., Weksberg, R. & Hamilton, J. Growth hormone deficiency in Costello syndrome. *Am. J. Med. Genet. A.* **129A,** 166–170 (2004).
45 Alexander, S., Ramadan, D., Alkhayyat, H., Al-Sharkawi, I., Backer, K. C., El-Sabban, F. *et al.* Costello syndrome and hyperinsulinemic hypoglycemia. *Am. J. Med. Genet. A.* **139,** 227–230 (2005).
46 Santoriello, C., Deflorian, G., Pezzimenti, F., Kawakami, K., Lanfrancone, L., d'Adda di Fagagna, F. *et al.* Expression of H-RASV12 in a zebrafish model of Costello syndrome causes cellular senescence in adult proliferating cells. *Dis. Model. Mech.* **2,** 56–67 (2009).
47 White, S. M., Graham, J. M. Jr, Kerr, B., Gripp, K., Weksberg, R., Cytrynbaum, C. *et al.* The adult phenotype in Costello syndrome. *Am. J. Med. Genet. A.* **136,** 128–135 (2005).
48 Seeburg, P. H., Colby, W. W., Capon, D. J., Goeddel, D. V. & Levinson, A. D. Biological properties of human c-Ha-ras1 genes mutated at codon 12. *Nature* **312,** 71–75 (1984).
49 Fasano, O., Aldrich, T., Tamanoi, F., Taparowsky, E., Furth, M. & Wigler, M. Analysis of the transforming potential of the human H-ras gene by random mutagenesis. *Proc. Natl Acad. Sci. USA* **81,** 4008–4012 (1984).
50 Jakobisiak, M. & Golab, J. Statins can modulate effectiveness of antitumor therapeutic modalities. *Med. Res. Rev.* **30,** 102–135 (2010).
51 Li, W., Cui, Y., Kushner, S. A., Brown, R. A., Jentsch, J. D., Frankland, P. W. *et al.* The HMG-CoA reductase inhibitor lovastatin reverses the learning and attention deficits in a mouse model of neurofibromatosis type 1. *Curr. Biol.* **15,** 1961–1967 (2005).
52 Krab, L. C., de Goede-Bolder, A., Aarsen, F. K., Pluijm, S. M., Bouman, M. J., van der Geest, J. N. *et al.* Effect of simvastatin on cognitive functioning in children with neurofibromatosis type 1: a randomized controlled trial. *JAMA* **300,** 287–294 (2008).
53 Dale, K. M., Coleman, C. I., Henyan, N. N., Kluger, J. & Whitem, C. M. Statins and cancer risk: a meta-analysis. *JAMA* **295,** 74–80 (2006).

Journal of Human Genetics (2011) 56, 34–40

www.nature.com/jhg

ORIGINAL ARTICLE

A genome-wide association study identifies *RNF213* as the first Moyamoya disease gene

Fumiaki Kamada[1], Yoko Aoki[1], Ayumi Narisawa[1,2], Yu Abe[1], Shoko Komatsuzaki[1], Atsuo Kikuchi[3], Junko Kanno[1], Tetsuya Niihori[1], Masao Ono[4], Naoto Ishii[5], Yuji Owada[6], Miki Fujimura[2], Yoichi Mashimo[7], Yoichi Suzuki[7], Akira Hata[7], Shigeru Tsuchiya[3], Teiji Tominaga[2], Yoichi Matsubara[1] and Shigeo Kure[1,3]

Moyamoya disease (MMD) shows progressive cerebral angiopathy characterized by bilateral internal carotid artery stenosis and abnormal collateral vessels. Although ~15% of MMD cases are familial, the MMD gene(s) remain unknown. A genome-wide association study of 785 720 single-nucleotide polymorphisms (SNPs) was performed, comparing 72 Japanese MMD patients with 45 Japanese controls and resulting in a strong association of chromosome 17q25-ter with MMD risk. This result was further confirmed by a locus-specific association study using 335 SNPs in the 17q25-ter region. A single haplotype consisting of seven SNPs at the *RNF213* locus was tightly associated with MMD ($P=5.3\times10^{-10}$). *RNF213* encodes a really interesting new gene finger protein with an AAA ATPase domain and is abundantly expressed in spleen and leukocytes. An RNA *in situ* hybridization analysis of mouse tissues indicated that mature lymphocytes express higher levels of *Rnf213* mRNA than their immature counterparts. Mutational analysis of *RNF213* revealed a founder mutation, p.R4859K, in 95% of MMD families, 73% of non-familial MMD cases and 1.4% of controls; this mutation greatly increases the risk of MMD ($P=1.2\times10^{-43}$, odds ratio=190.8, 95% confidence interval=71.7–507.9). Three additional missense mutations were identified in the p.R4859K-negative patients. These results indicate that *RNF213* is the first identified susceptibility gene for MMD.
Journal of Human Genetics (2011) **56**, 34–40; doi:10.1038/jhg.2010.132; published online 4 November 2010

INTRODUCTION

'Moyamoya' is a Japanese expression for something hazy, such as a puff of cigarette smoke drifting in the air. In individuals with Moyamoya disease (MMD), there is a progressive stenosis of the internal carotid arteries; a fine network of collateral vessels, which resembles a puff of smoke on a cerebral angiogram, develops at the base of the brain (Figure 1a).[1,2] This steno-occlusive change can cause transient ischemic attacks and/or cerebral infarction, and rupture of the collateral vessels can cause intracranial hemorrhage. Children under 10 years of age account for nearly 50% of all MMD cases.[3]

The etiology of MMD remains unclear, although epidemiological studies suggest that bacterial or viral infection may be implicated in the development of the disease.[4] Growing attention has been paid to the upregulation of arteriogenesis and angiogenesis associated with MMD because chronic ischemia in other disease conditions is not always associated with a massive development of collateral vessels.[5,6] Several angiogenic growth factors are thought to have functions in the development of MMD.[7]

Several lines of evidence support the importance of genetic factors in susceptibility to MMD.[8] First, 10–15% of individuals with MMD have a family history of the disease.[9] Second, the concordance rate of MMD in monozygotic twins is as high as 80%.[10] Third, the prevalence of MMD is 10 times higher in East Asia, especially in Japan (6 per 100 000 population), than in Western countries.[3] Familial MMD may be inherited in an autosomal dominant fashion with low penetrance or in a polygenic manner.[11] Linkage studies of MMD families have revealed five candidate loci for an MMD gene: chromosomes 3p24–26,[12] 6q25,[13] 8q13–24,[10] 12p12–13[10] and 17q25.[14] However, no susceptibility gene for MMD has been identified to date.

We collected 20 familial cases of MMD to investigate linkage in the five putative MMD loci. However, a definitive result was not obtained for any of the loci. We then hypothesized that there might be a founder mutation among Japanese patients with MMD because the prevalence of MMD is unusually high in Japan.[15] Genome-wide and locus-specific association studies were performed and successfully identified a single gene, *RNF213*, linked to MMD. We report here a strong association between MMD onset and a founder mutation in *RNF213*, as well as the expression profiles of *RNF213*, in various tissues.

[1]Department of Medical Genetics, Tohoku University School of Medicine, Sendai, Japan; [2]Department of Neurosurgery, Tohoku University School of Medicine, Sendai, Japan; [3]Department of Pediatrics, Tohoku University School of Medicine, Sendai, Japan; [4]Department of Pathology, Tohoku University School of Medicine, Sendai, Japan; [5]Department of Microbiology and Immunology, Tohoku University School of Medicine, Sendai, Japan; [6]Department of Organ Anatomy, Yamaguchi University Graduate School of Medicine, Ube, Japan and [7]Department of Public Health, Graduate School of Medicine, Chiba University, Chiba, Japan
Correspondence: Dr S Kure, Department of Pediatrics, Tohoku University School of Medicine, 1-1 Seiryo-machi, Aoba-ku, Miyagi, Sendai 980-8574, Japan.
E-mail; kure@med.tohoku.ac.jp
Received 30 September 2010; accepted 1 October 2010; published online 4 November 2010

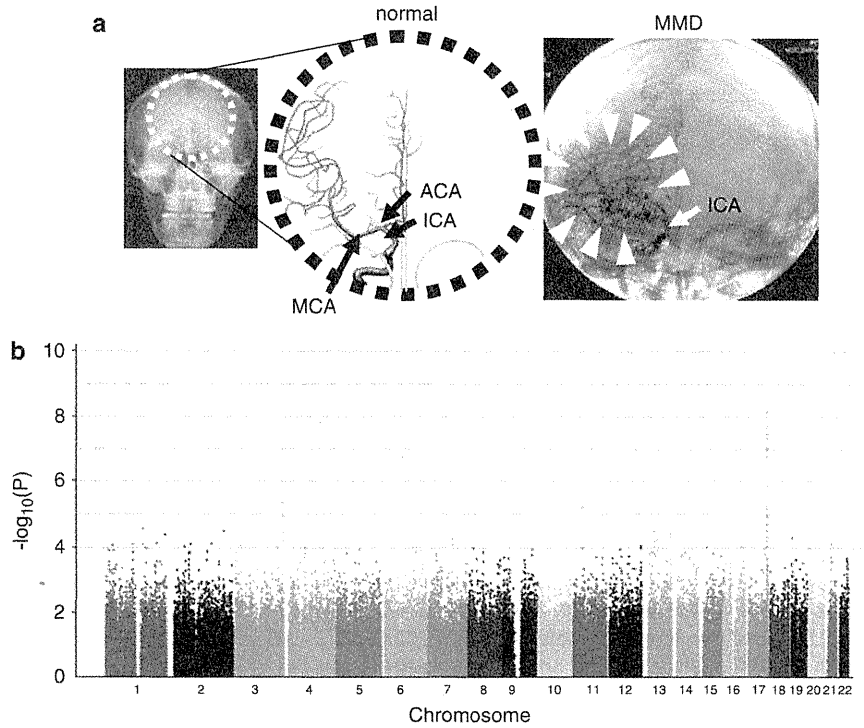

Figure 1 (**a**) Abnormal brain vessels in MMD. The dotted circle indicates the X-ray field of cerebral angiography (left panel). Normal structures of the right internal carotid artery (ICA), anterior cerebral artery (ACA) and middle cerebral artery (MCA) are illustrated (middle panel). The arrowheads indicate abnormal collateral vessels appearing like a puff of smoke in the angiogram of an individual with MMD (right panel). Note that ACA and MCA are barely visible, because of the occlusion of the terminal portion of the ICA. (**b**) Manhattan plot of the 785 720 SNPs used in the genome-wide association analysis of MMD patients. Note that the SNPs in the 17q25-ter region reach a significance of $P<10^{-8}$.

MATERIALS AND METHODS

Affected individuals

Genomic DNA was extracted from blood and/or saliva samples obtained from members of the families with MMD (Supplementary Figure 1), MMD patients with no family history and control subjects. All of the subjects were Japanese. MMD was diagnosed on the basis of guidelines established by the Research Committee on Spontaneous Occlusion of the Circle of Willis of the Ministry of Health and Welfare of Japan. This study was approved by the Ethics Committee of Tohoku University School of Medicine. Total RNA samples were purified from leukocytes using an RNeasy mini kit (Qiagen, Hilden, Germany) and used as templates for cDNA synthesis with an Oligo $(dT)_{20}$ primer and SuperScript II reverse transcriptase according to the manufacturer's instructions (Invitrogen, Carlsbad, CA, USA).

Linkage analysis

For the linkage analysis, DNA samples were genotyped for 36 microsatellite markers within five previously reported MMD loci using the ABI 373A DNA Sequencer (Applied Biosystems, Foster City, CA, USA). Pedigrees and haplotypes were constructed with the Cyrillic version 2.1 software (Oxfordshire, UK). Multipoint analyses were conducted using the GENEHUNTER 2 software (http://www.broadinstitute.org/ftp/distribution/software/genehunter/). Statistical analysis was performed with SPSS version 14.0J (SPSS, Tokyo, Japan).

Genome-wide and locus-specific association studies

A genome-wide association study was performed using a group of 72 MMD patients, which consisted of 64 patients without a family history of MMD and 8 probands of MMD families. The Illumina Human Omni-Quad 1 chip (Illumina, San Diego, CA, USA) was used for genotyping, and single-nucleotide polymorphisms (SNPs) with a genotyping completion rate of 100% were used for further statistical analysis (785 720 out of 1 140 419 SNPs). Genotyping data from 45 healthy Japanese controls were obtained from the database at the International HapMap Project web site. The 785 720 SNPs were statistically analyzed using the PLINK software (http://pngu.mgh.harvard.edu/~purcell/plink/index.shtml). For a locus-specific association study, we used 63 DNA samples consisting of 58 non-familial MMD patients and 5 probands of MMD families. A total of 384 SNPs within chromosome 17q25-ter were genotyped (Supplementary Table 1), using the GoldenGate Assay and a custom SNP chip (Illumina). Genotyping data for 45 healthy Japanese were used as a control. Case–control single-marker analysis, haplotype frequency estimation and significance testing of differences in haplotype frequency were performed using the Haploview version 3.32 program (http://www.broad.mit.edu/mpg/haploview/).

Mutation detection

Mutational analyses of *RNF213* and *FLJ35220* were performed by PCR amplification of each coding exon and putative promoter regions, followed by direct sequencing. Genomic sequence data for the two genes were obtained from the National Center for Biotechnology Information web site (http://www.ncbi.nlm.nih.gov/) for design of exon-specific PCR primers. *RNF213* cDNA fragments were amplified from leukocyte mRNA for sequencing analysis. Sequencing of the PCR products was performed with the ABI BigDye Terminator Cycle Sequencing Reaction Kit using the ABI 310 Genetic Analyzer. Identified base changes were screened in control subjects. Statistical difference of the carrier frequency of each base change was estimated by Fisher's exact test (the MMD group vs the control group).

Quantitative PCR

MTC Multiple Tissue cDNA Panels (Clontech Laboratory, Madison, WI, USA) were the source of cDNAs from human cell lines, adult and fetal tissues. Mononuclear cells and polymorphonuclear cells were isolated from the fresh peripheral blood of healthy human adults using Polymorphprep (Cosmo Bio,

Carlsbad, CA, USA). T and B cells were isolated from the fresh peripheral blood of healthy human adults using the autoMACS separator (Militeny Biotec, Bergisch Gladbach, Germany). Total RNA was isolated from these cells with the RNeasy Mini Kit (Qiagen) following the manufacturer's instructions. We reverse transcribed 100 ng samples of total RNA into cDNAs using the High Capacity cDNA Reverse Transcription Kit (Applied Biosystems). Quantitative PCRs were performed in a final volume of 20 μl using the FastStart TaqMan Probe Master (Rox) (Roche, Madison, WI, USA), 5 μl of cDNA, 10 μM of *RNF*- or *GAPDH*-specific primers and 10 μM of probes (Universal ProbeLibrary Probe #80 for *RNF213* and Roche Probe #60 for *GAPDH*). All reactions were performed in triplicate using the ABI 7500 Real-Time PCR system (Applied Biosystems). Cycling conditions were 2 min at 50°C and 10 min at 95°C, followed by 40 cycles of 15 s at 95°C and 60 s at 60°C. Real-time PCR data were analyzed by the SDS version 1.2.1 software (Applied Biosystems). We evaluated the relative level of *RNF213* mRNA by determining the C_T value, the PCR cycle at which the reporter fluorescence exceeded the signal baseline. *GAPDH* mRNA was used as an internal reference for normalization of the quantitative expression values.

Multiplex PCR

MTC Multiple Tissue cDNA Panels (Clontech) were the source of human cell lines and cDNAs from human adult and fetal tissues. Multiplex PCRs were performed in a final volume of 20 μl using the Multiplex PCR Master Mix (Qiagen), 2 μl of cDNA, a 2 μM concentration of *RNF213* and a 10 μM concentration of *GAPDH*-specific primers. The samples were separated on a 2% agarose gel stained with ethidium bromide. Cycling conditions were 15 min at 94°C, followed by 30 cycles of 30 s at 94 °C, 30 s at 57 °C and 30 s at 72 °C. For normalization of the expression levels, we used *GAPDH* as an internal reference for each sample.

In situ hybridization (ISH) analysis

Paraffin-embedded blocks and sections of mouse tissues for ISH were obtained from Genostaff (Tokyo, Japan). The mouse tissues were dissected, fixed with Tissue Fixative (Genostaff), embedded in paraffin by proprietary procedures (Genostaff) and sectioned at 6 μm. To generate anti-sense and sense RNA probes, a 521-bp DNA fragment corresponding to nucleotide positions 470–990 of mouse *Rnf213* (BC038025) was subcloned into the pGEM-T Easy vector (Promega, Madison, WI, USA). Hybridization was performed with digoxigenin-labeled RNA probes at concentrations of 300 ng ml^{-1} in Probe Diluent-1 (Genostaff) at 60 °C for 16 h. Coloring reactions were performed with NBT/BCIP solution (Sigma-Aldrich, St Louis, MO, USA). The sections were counterstained with Kernechtrot stain solution (Mutoh, Tokyo, Japan), dehydrated and mounted with Malinol (Mutoh). For observation of *Rnf213* expression in activated lymphocytes, 10-week-old Balb/c mice were intraperitoneally injected with 100 μg of keyhole limpet hemocyanin and incomplete adjuvant and sacrificed in 2 weeks. The spleen of the mice was removed for Hematoxylin–eosin staining and ISH analyses.

RESULTS

Using 20 Japanese MMD families, we reevaluated the linkage mapped previously to five putative MMD loci. No locus with significant linkage, Lod score >3.0 or NPL score >4.0 was confirmed (Supplementary Figure 2). We conducted a genome-wide association study of 72 Japanese MMD cases. Single-marker allelic tests comparing the 72 MMD cases and 45 controls were performed for 785 720 SNPs using χ^2 statistics. These tests identified a single locus with a strong association with MMD ($P<10^{-8}$) on chromosome 17q25-ter (Figure 1b), which is in line with the latest mapping data of a MMD locus.[16] The SNP markers with $P<10^{-6}$ are listed in Table 1. To confirm this observation, we performed a locus-specific association study. A total of 384 SNP markers (Supplementary Table 1) were selected within the chromosome 17q25-ter region and genotyped in a set of 63 MMD cases and 45 controls. The SNP markers demonstrating a high association with MMD ($P<10^{-6}$) were clustered in a 151-kb region from base position 75 851 399–76 003 020 (SNP No.116–136 in

Table 1 A genome-wide association study of Japanese MMD patients and controls

	SNP	*Chromosome*	*Base position*	*Gene*	*Risk allele/ non-risk allele*	*Risk allele frequency in MMD*	*Risk allele frequency in controls*	χ^2	*P-value*	*Odds ratio*	*95% confidence interval*	
											Lower	*Upper*
1	rs11870849	17	76 025 668	*RNF213*	T/C	0.4792	0.1111	33.55	6.95E-09	7.36	3.532	15.34
2	rs6565681	17	75 963 089	*RNF213*	A/G	0.7361	0.3667	31.35	2.16E-08	4.819	2.733	8.489
3	rs7216493	17	75 941 953	*RNF213*	G/A	0.75	0.3889	30.39	3.53E-08	4.715	2.673	8.313
4	rs7217421	17	75 850 055	*RNF213*	A/G	0.6667	0.3	29.86	4.64E-08	4.666	2.642	8.237
5	rs12449863	17	75 857 806	*RNF213*	C/T	0.6667	0.3	29.86	4.64E-08	4.666	2.642	8.237
6	rs4890009	17	75 926 103	*RNF213*	G/A	0.8819	0.5778	28.5	9.38E-08	5.459	2.831	10.527
7	SNP17-75933731	17	75 933 731	*RNF213*	G/A	0.8819	0.5778	28.5	9.38E-08	5.458	2.831	10.527
8	rs7219131	17	75 867 365	*RNF213*	T/C	0.6667	0.3111	28.11	1.15E-07	4.429	2.517	7.794
9	rs6565677	17	75 932 037	*RNF213*	T/C	0.7431	0.3977	27.43	1.63E-07	4.378	2.483	7.722
10	rs4889848	17	75 969 256	*RNF213*	C/T	0.75	0.4111	26.99	2.05E-07	4.297	2.444	7.889
11	rs7224239	17	75 969 771	*RNF213*	A/G	0.8681	0.5667	26.99	2.05E-07	5.03	2.659	9.529

Abbreviations: MMD, moyamoya disease; SNP, single-nucleotide polymorphism.A genome-wide association study testing 1 140 419 SNPs on the Human Omni-Quad 1chip (Illumina, San Diego, CA, USA) was performed in 72 Japanese MMD cases. Single-marker allelic tests between the cases and controls were performed using χ^2 statistics for all markers. This table lists the 11 SNP markers with a significance of $P<10^{-6}$.

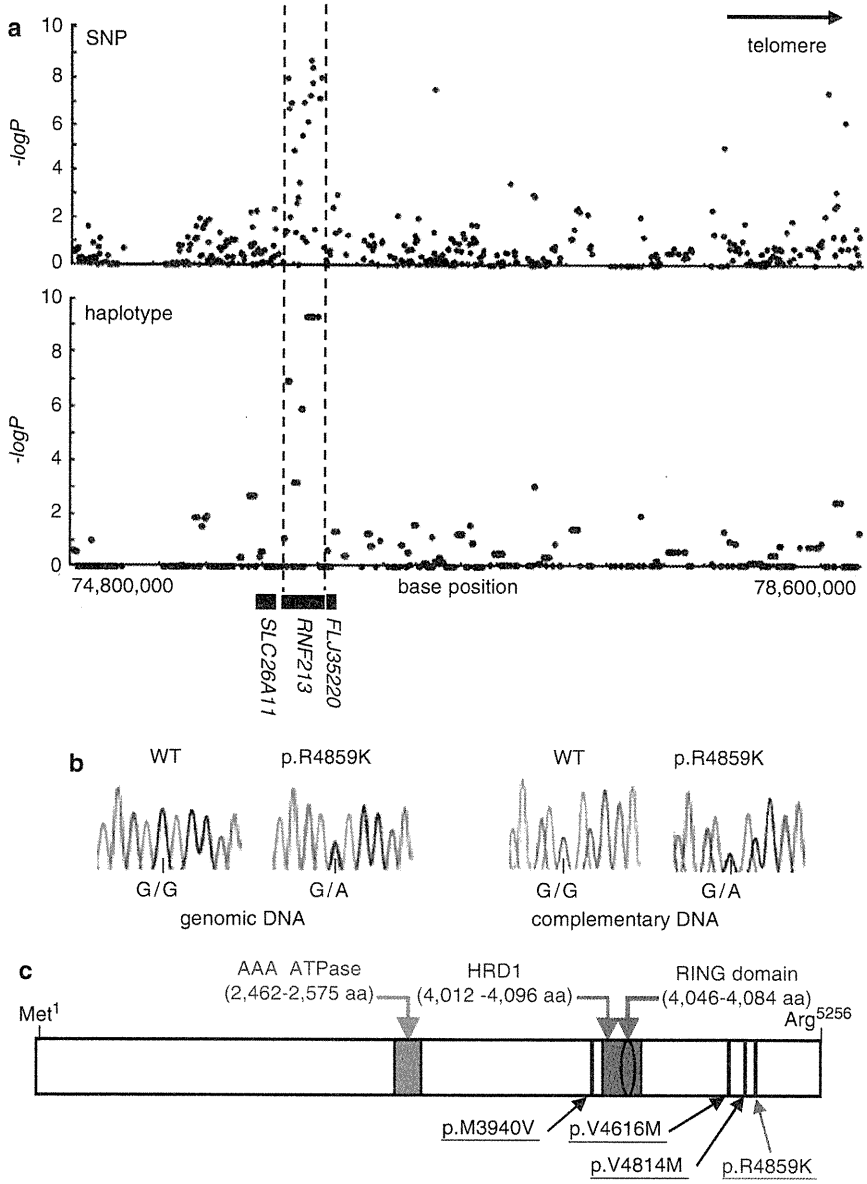

Figure 2 (**a**) Association analysis of 63 non-familial MMD cases and 45 control subjects. Statistical significance was evaluated by the χ^2-test. SNP markers with a strong association with MMD ($P<10^{-6}$) clustered in a 161-kb region (base position 75 851 399–76 012 838) indicated by two dotted lines (upper panel), which included the entire region of *RNF213* (lower panel). Haplotype analysis revealed a strong association ($P=5.3\times10^{-10}$) between MMD and a single haplotype located within *RNF213*. (**b**) Sequencing chromatograms of the identified MMD mutations. The left panel shows the sequences of an unaffected individual and a carrier of a p.R4859K heterozygous mutation. The right panel indicates the sequencing chromatograms of the leukocyte cDNA obtained from an unaffected individual and an individual with MMD who carries the p.R4859K mutation. Note that both wild-type and mutant alleles were expressed in leukocytes. (**c**) The structure of the RNF213 protein. The RNF213 protein contains three characteristic structures, the AAA-superfamily ATPase motif, the RING motif and the HMG-CoA reductase degradation motif. The positions of four mutations identified in MMD patients are underlined, including one prevalent mutation (red) and three private mutations (black).

Supplementary Table 1); this entire region was within the *RNF213* locus (Figure 2a). A single haplotype determined by seven SNPs (SNP Nos.130–136 in Supplementary Table 1) that resided in the 3′ region of *RNF213* was strongly associated with MMD onset ($P=5.3\times10^{-10}$). Analysis of the linkage disequilibrium block indicated that this haplotype was not in complete linkage disequilibrium with any other haplotype in this region (Supplementary Figure 3). These results strongly suggest that a founder mutation may exist in the 3′ part of *RNF213*.

Mutational analysis of the entire coding and promoter regions of *RNF213* and *FLJ35220*, a gene 3′ adjacent to *RNF213*, revealed that 19 of the 20 MMD families shared the same single base substitution, c.14576G>A, in exon 60 of *RNF213* (Figure 2b and Table 2). This nucleotide change causes an amino-acid substitution from arginine^{4859} to lysine^{4859} (p.R4859K). The p.R4859K mutation was identified in 46 of 63 non-familial MMD cases (73%), including 45 heterozygotes and a single homozygote (Table 3). Both the wild-type and the p.R4859K mutant alleles were co-expressed in leukocytes

Table 2 Nucleotide changes with amino-acid substitutions identified in the sequencing analysis of *RNF213* and *FLJ35220*

			Genotype (allele)				
Gene	*Exon*	*Nucleotide change[a] (amino-acid substitution)*	*Non-familial cases*	*Control subjects*	*P-value[b]*	*χ^2 (df=1) [c]*	*Odds ratio (95% CI)*
RNF213	29	c.7809C>A (p.D2603E)	2/63 (2/126)	15/381 (15/762)	0.77	0.09	0.80 (0.2–3.6)
RNF213	41	c.11818A>G (p.M3940V)	1/63 (1/126)	0/388 (0/776)	0.01	6.17	ND
RNF213	41	c.11891A>G (p.E3964G)	4/63 (4/126)	3/55 (4/110)	0.84	0.04	1.2 (0.3–5.5)
RNF213	52	c.13342G>A (p.A4448T)	4/63 (4/126)	2/53 (2/106)	0.53	0.39	1.7 (0.3–9.8)
RNF213	56	c.13846G>A (p.V4616M)	1/63 (1/126)	0/388 (0/776)	0.01	6.17	ND
RNF213	59	c.14440G>A (p.V4814M)	1/63 (1/126)	0/388 (0/776)	0.01	6.17	ND
RNF213	60	c.14576G>A (p.R4859K)	46/63 (47/126)	6/429 (6/858)	1.2×10^{-43}	298.1	190.8 (71.7–507.9)
FLJ35220		None					

Abbreviations: ND, not determined; SNP, single-nucleotide polymorphism.
[a]Nucleotide numbers of *RNF213* cDNA are counted from the A of the ATG initiator methionine codon (NCBI Reference sequence, NP_065965.4).
[b]*P*-values were calculated by Fisher's exact test.
[c]Genotypic distribution (carrier of the polymorphism vs non-carrier).

Table 3 Association of the p.R4859K (c.14576G>A) mutation with MMD

		Genotype		
	Total	*wt/wt (%)*	*wt/p.R4859K (%)*	*p.R4859K/ p.R4859K (%)[d]*
Members of 19 MMD families[a]				
Affected	42	0	39 (92.9)	3 (7.1)
Not affected	28	15 (53.6)	13 (46.4)	0
Individuals without a family history of MMD[b,c]				
Affected	63	17 (27.0)	45 (71.4)	1 (1.6)
Not affected	429	423 (98.6)	6 (1.4)	0

Abbreviations: MMD, moyamoya disease.
[a]Entire distribution, $\chi^2=29.4$, $P=4.2\times10^{-7}$.
[b]Entire distribution, $\chi^2=298.2$, $P=1.8\times10^{-65}$.
[c]Genotypic distribution (p.R4859K carrier vs non-carrier), $\chi^2=298.1$, $P=1.2\times10^{-43}$, odds ratio=190.8 (95% CI=71.7–507.9).
[d]The age of onset and initial symptoms of the four homozygotes were comparable to those of the 84 heterozygous patients.

in three patients heterozygous for the p.R4859K mutation (Figure 2b), excluding the possible instability of the mutant *RNF213* mRNA. Additional missense mutations, p.M3940V, p.V4616M and p.V4814M, were detected in three non-familial MMD cases without the p.R4859K mutation (Figure 2c). These mutations were not found in 388 control subjects and were detected in only one patient, suggesting that they were private mutations (Table 2). No copy number variation or mutation was identified in the *RNF213* locus of 12 MMD patients using comparative genome hybridization microarray analysis (Supplementary Figure 4). In total, 6 of the 429 control subjects (1.4%) were found to be heterozygous carriers of p.R4859K. Therefore, we concluded that the p.R4859K mutation increases the risk of MMD by a remarkably high amount (odds ratio=190.8 (95% confidence interval=71.7–507.9), $P=1.2\times10^{-43}$) (Table 3). It was recently reported that an SNP (ss161110142) in the promoter region of *RPTOR*, which is located ~150 kb downstream from *RNF213*, was associated with MMD.[17] Genotyping of the SNP in *RPTOR* showed that the *RNF213* p.R4859K mutation was more strongly associated with MMD than ss161110142 (Supplementary Figure 1).

RNF213 encodes a protein with 5256 amino acids harboring a RING (really interesting new gene) finger motif, suggesting that it functions as an E3 ubiquitin ligase (Figure 2c). It also has an AAA ATPase domain, which is characteristic of energy-dependent unfoldases.[18] To our knowledge, RNF213 is the first RING finger protein known to contain an AAA ATPase domain. The expression profile of *RNF213* has not been previously fully characterized. We performed a quantitative reverse transcription PCR analysis in various human tissues and cells. *RNF213* mRNA was highly expressed in immune tissues, such as spleen and leukocytes (Figure 3a and Supplementary Figure 5). Expression of *RNF213* was detected in fractions of both polymorphonuclear cells and mononuclear cells and was found in both B and T cell fractions (Supplementary Figure 6). A low but significant expression of *RNF213* was also observed in human umbilical vein endothelial cells and human pulmonary artery smooth muscle cells. Cellular expression was not enhanced in tumor cell lines, compared with leukocytes. In human fetal tissues, the highest expression was observed in leukocytes and the thymus (Supplementary Figure 6E). The expression of *RNF213* was surprisingly low in both adult and fetal brains. Overall, *RNF213* was ubiquitously expressed, and the highest expression was observed in immune tissues.

We studied the cellular expression of *Rnf213* in mice. The ISH analysis of spleen showed that *Rnf213* mRNA was present in small mononuclear cells, which were mainly localized in the white pulps (Figures 3b–g). The ISH signals were also detected in the primary follicles in the lymph node and in thymocytes in the medulla of the thymus (Supplementary Figure 7). To study *Rnf213* expression in activated lymphocytes we immunized mice with keyhole limpet hemocyanin, and examined *Rnf213* mRNA in spleen by ISH analysis. Primary immunization with keyhole limpet hemocyanin antigen revealed that the expression of *Rnf213* in the secondary follicle is as high as in the primary follicle in the lymph node (Supplementary Figure 8). In an E16.5 mouse embryo, expression was observed in the medulla of the thymus and in the cells around the mucous palatine glands (Supplementary Figure 9). These findings suggest that mature lymphocytes in a static state express *Rnf213* mRNA at a higher level than do their immature counterparts.

DISCUSSION

We identified a susceptibility locus for MMD by genome-wide and locus-specific association studies. Further sequencing analysis revealed a founder missense mutation in *RNF213*, p.R4859K, which was tightly associated with MMD onset. Identification of a founder mutation in individuals with MMD would resolve the following recurrent